JACS
JOURNAL OF THE AMERICAN CHEMICAL SOCIETY

ARTICLE

pubs.acs.org/JACS

Small Molecule Activation by Uranium Tris(aryloxides): Experimental and Computational Studies of Binding of N_2, Coupling of CO, and Deoxygenation Insertion of CO_2 under Ambient Conditions

Stephen M. Mansell,[†] Nikolas Kaltsoyannis,[*,‡] and Polly L. Arnold[*,†]

[†]EaStCHEM School of Chemistry, University of Edinburgh, Joseph Black Building, The King's Buildings, Edinburgh, EH9 3JJ, U.K.
[‡]Department of Chemistry, University College London, 20 Gordon Street, London, WC1H 0AJ, U.K.

Supporting Information

ABSTRACT: Previously unanticipated dinitrogen activation is exhibited by the well-known uranium tris(aryloxide) $U(ODtbp)_3$, $U(OC_6H_3\text{-}Bu^t_2\text{-}2,6)_3$, and the tri-*tert*-butyl analogue $U(OTtbp)_3$, $U(OC_6H_2\text{-}Bu^t_3\text{-}2,4,6)_3$, in the form of bridging, side-on dinitrogen complexes $[U(OAr)_3]_2(\mu\text{-}\eta^2\text{:}\eta^2\text{-}N_2)$, for which the tri-*tert*-butyl N_2 complex is the most robust $U_2(N_2)$ complex isolated to date. Attempted reduction of the tris(aryloxide) complex under N_2 gave only the potassium salt of the uranium(III) tetra(aryloxide) anion, $K[U(OAr)_4]$, as a result of ligand redistribution. The solid-state structure is a polymeric chain formed by each potassium cation bridging two arenes of adjacent anions in an η^6 fashion. The same uranium tris(aryloxides) were also found to couple carbon monoxide under ambient conditions to give exclusively the ynediolate $[OCCO]^{2-}$ dianion in $[U(OAr)_3]_2(\mu\text{-}\eta^1\text{:}\eta^1\text{-}C_2O_2)$, in direct analogy with the reductive coupling recently shown to afford $[U\{N(SiMe_3)_2\}_3]_2(\mu\text{-}\eta^1\text{:}\eta^1\text{-}C_2O_2)$. The related U^{III} complexes $U\{N(SiPhMe_2)_2\}_3$ and $U\{CH(SiMe_3)_2\}_3$ however do not show CO coupling chemistry in our hands. Of the aryloxide complexes, only the $U(OC_6H_2\text{-}Bu^t_3\text{-}2,4,6)_3$ reacts with CO_2 to give an insertion product containing bridging oxo and aryl carbonate moieties, $U_2(OTtbp)_4(\mu\text{-}O)(\mu\text{-}\eta^1\text{:}\eta^1\text{-}O_2COC_6H_2\text{-}Bu^t_3\text{-}2,4,6)_2$, which has been structurally characterized. The presence of coordinated N_2 in $[U(OTtbp)_3]_2(N_2)$ prevents the occurrence of any reaction with CO_2, underscoring the remarkable stability of the N_2 complex. The di-*tert*-butyl aryloxide does not insert CO_2, and only $U(ODtbp)_4$ was isolated. The silylamide also reacts with carbon dioxide to afford $U(OSiMe_3)_4$ as the only uranium-containing material. GGA and hybrid DFT calculations, in conjunction with topological analysis of the electron density, suggest that the U−N_2 bond is strongly polar, and that the only covalent U→N_2 interaction is π backbonding, leading to a formal $(U^{IV})_2(N_2)^{2-}$ description of the electronic structure. The N−N stretching wavenumber is preferred as a metric of N_2 reduction to the N−N bond length, as there is excellent agreement between theory and experiment for the former but poorer agreement for the latter due to X-ray crystallographic underestimation of r(N−N). Possible intermediates on the CO coupling pathway to $[U(OAr)_3]_2(\mu\text{-}C_2O_2)$ are identified, and potential energy surface scans indicate that the ynediolate fragment is more weakly bound than the ancillary ligands, which may have implications in the development of low-temperature and pressure catalytic CO chemistry.

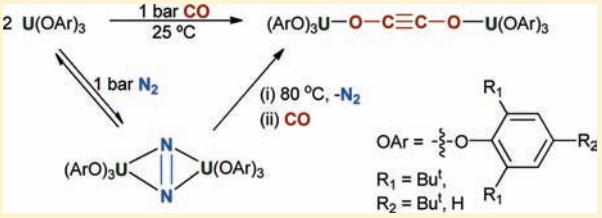

INTRODUCTION

Carbon monoxide and dinitrogen are the two diatomic molecules which have the strongest bonds found in the Periodic Table (1076.5 ± 0.4 kJ mol^{-1} and 945.33 ± 0.59 kJ mol^{-1}, respectively).[1] Despite this, dinitrogen is the source of nitrogen atoms for both biological systems[2,3] and the chemical industry,[4] while carbon monoxide is an important C_1 feedstock for conversion into larger molecules in industrial processes.[5] In nature, dinitrogen is reduced by nitrogenase enzymes involving active sites that include a MoFe metal core as the active site.[3,6] In industry, the well-known Haber−Bosch process produces 100 million tons of ammonia per year, a scale that is thought to be similar to that observed in nature,[7] using heterogeneous catalysts based on iron or ruthenium and at a huge energetic cost (350−550 °C and 150−350 atm).[8] The Fischer−Tropsch process uses carbon monoxide and dihydrogen as feedstocks to produce alkanes and alkenes for use as fuels and bulk chemicals.[9,10] The catalysts used are heterogeneous and are based on cobalt or iron, and the process requires temperatures (200−350 °C) and pressures significantly (20−44 atm) above ambient.[9]

Industrially viable homogeneous Haber−Bosch or Fischer−Tropsch processes that work under mild conditions have yet to be realized,[10,11] although there have been some significant advances in the further reactivity of metal-ligated dinitrogen and carbon monoxide.[12] Examples of N_2 reactions with group 4 metals include the reaction of bridging, side-on bound dinitrogen coordinated to zirconium with dihydrogen and primary silanes,[13] the reaction of a C_5Me_4H zirconium N_2 complex with H_2 to form NH_3,[14] a Hf analogue with CO to form addition products,[15] and

Received: March 8, 2011
Published: May 17, 2011

the catalytic reduction of N_2 to NH_3 occurring with a few turnovers at a single Mo center.[8,16] f-Element dinitrogen chemistry remains poorly developed in comparison. The highly contracted nature of the 4f orbitals leads to almost no orbital contribution to lanthanide coordination chemistry, and therefore binding of classical ligands used in transition metal chemistry, such as N_2 and CO, was not anticipated. The complex $[(C_5Me_5)_2Sm]$ was the first f-element complex shown to bind N_2, but the N_2 is easily displaced, and in solution the N_2-bound and non-N_2 bound species are in equilibrium.[17] Since then, more reducing Ln(II) complexes have been used, aiding N_2 binding by partially reducing the N_2 ligand.[18,19] The combination of LnA_3 (A = $N(SiMe_3)_2$, (C_5Me_5), (C_5Me_4H), OC_6H_3-Bu^t-2,6) and a strong reductant such as Na or KC_8 leads to dinitrogen reduction if the Ln does not have an available +II oxidation state, affording $\{A_2(THF)Ln\}_2(\mu\text{-}\eta^2\text{:}\eta^2\text{-}N_2)$ in yields that can vary because other reduction products are formed in some cases.[20,21] Particularly notable was the isolation of the unusual N_2^{3-} as a ligand from the reaction of $Y\{N(SiMe_3)_2\}_3$ with K under N_2 or the reaction of DyI_2 + 2 KOAr under N_2.[22,23] Even a scandium N_2 complex $[(C_5Me_4H)_2Sc]_2(\mu\text{-}\eta^2\text{:}\eta^2\text{-}N_2)$ has recently been reported.[24]

The 5f orbitals are not as contracted as the 4f orbitals, which leads to greater orbital participation in actinide bonding with the potential for actinide compounds to access different chemistry to the lanthanides. Only four molecular dinitrogen uranium complexes have been reported, although side-on binding is increasingly found in electropositive metal systems.[25] The side-on binding of N_2 in the seminal tren complex $[UN(NCH_2CH_2NSiBu^tMe_2)_3]_2(\mu\text{-}\eta^2\text{:}\eta^2\text{-}N_2)$ occurs at ambient pressure and is reversed by freeze−pump−thaw degassing of solutions;[26] 5 psi pressures are required to crystallize $[U(\eta\text{-}Cp^*)(\eta\text{-}C_8H_4\{Si^iPr_3\text{-}1,4\}_2)]_2(\mu\text{-}\eta^2\text{:}\eta^2\text{-}N_2)$ despite the formal reduction to diazenido (N_2^{2-}),[27] and 80 psi pressures of N_2 are required to stabilize $U(\eta\text{-}Cp^*)_3(N_2)$,[28] whereas additional reduction from Mo^{III} allows the isolation of $\{C_6H_3Me_2\text{-}3,5(Bu^t)N\}_3U(\mu\text{-}\eta^1\text{:}\eta^1\text{-}N_2)Mo\{N(Bu^t)Ph\}_3$.[29] Gambarrota and co-workers have also reported the crystal structure of a bridging dinitrido U^{IV}/U^V complex from the reduction of a uranium(III) tetrapyrrole compound under dinitrogen using potassium naphthalide as an external reducing reagent.[30] Interestingly, it has been observed that uranium is an efficient catalyst in the Haber−Bosch process,[31] and hence these initial results are of great potential interest.[32]

While many metal complexes are capable of inserting CO into a M−E bond, very few can mediate the C−C coupling of CO. With transition metal systems, $[M(CO)_2(dmpe)_2Cl]$ (M = Nb, Ta) can be reduced with magnesium in the presence of Cp_2ZrCl_2 or with Na/Hg followed by addition of Me_3SiCl to afford coupled and silylated $[M(Me_3SiOC{\equiv}COSiMe_3)(dmpe)_2Cl]$ (M = Nb, Ta; dmpe =1,2-bis{dimethylphosphino}ethane).[33] The Ta compound can also be protonated to give coordinated HOC≡COH.[34] Insertion of 1 and 2 equiv of CO into the weak Rh−Rh bond in the rhodium octaethylporphyrin (oep) dimer $[Rh(oep)]_2$ has been observed, and 12 atm pressures of CO were used to force the equilibrium reaction over to a double insertion product characterized by NMR spectroscopy as $[(oep)Rh(CO)(CO)Rh(oep)]$.[35] A ditantalum hydride with a supporting tridentate, trisaryloxide ligand was recently found to reductively couple six CO molecules, giving a chain of six carbon atoms containing alternate single and double bonds in $[Ta(2,6\text{-}(CH_2\text{-}3\text{-}^tBu\text{-}5\text{-}Me\text{-}2\text{-}OPh)(thf)]_4(C_6O_6)$.[36] It is known that alkali metals react with CO to form ill-defined MOCCOM materials, but these are shock-sensitive and can be thermally unstable.[37]

In f-element chemistry, CO has been reductively homologated by the strongly reducing La^{III} and Sm^{II} complexes, $[La(\eta\text{-}Cp^*)_2]_2(\mu\text{-}N_2)$ and $[Sm(\eta\text{-}Cp^*)_2(thf)_2]$, affording a ketene carboxylate dianion from three CO molecules at 90 psi pressures in moderate isolated yields.[17,38] Binding of CO to uranium(III) was first demonstrated in $[(Me_3SiC_5H_4)_3U(CO)]$ with ν_{CO} 1922 cm^{-1},[39] and since for other tris(cyclopentadienyl) derivatives,[39−41] and for the chelating aryloxide complex $[\{(^{tBu}ArO)_3tacn\}U]_2(CO)$ ($\{(^{tBu}ArO)_3tacn\} = \{C_6H_{12}[NCH_2C_6H_2Bu^t\text{-}3,5\text{-}O))_3\}$),[42] but reductive coupling has been demonstrated only in the past few years, and for three systems: The sterically congested, trivalent, organometallic uranium complexes $U(\eta\text{-}C_8H_6\{SiPr^i_3\text{-}1,4\}_2)(\eta^5\text{-}Cp^R)]$ ($Cp^R = C_5(CH_3)_5$ or $C_5(CH_3)_4H$) can reductively homologate CO to form the deltate dianion,[43] squarate dianion,[44] or if exactly 1 equiv of CO is used per U, the ynediolate dianion.[45] We recently showed a CO coupling reaction that exclusively forms the ynediolate dianion from a simple uranium starting material, $U\{N(SiMe_3)_2\}_3$, using an excess of CO at ambient temperature and pressure, and that heating the resultant complex $[U\{N(SiMe_3)_2\}_3]_2(\mu\text{-}\eta^1\text{:}\eta^1\text{-}OCCO)$, resulted in the formal addition of a silylmethyl C−H bond across the CC triple bond.[46]

f-Element complexes are also capable of carbon dioxide reduction and activation. Most commonly, insertion into a M−E σ-bond occurs, forming esters, carbonates, or carbamates, according to the nature of E (C, O, N). For reducing f-element complexes, deoxygenation is also regularly seen, converting M^{III} complexes to M^{IV}−O−M^{IV} complexes,[47] with the CO usually not identified in the products, except in one example in which a particularly encumbered ligand system allows both $[\{(^RArO)_3tacn\}U]_2(\eta^1\text{-}CO)$ (R = Bu^t) and the μ-O adduct to be isolated,[42,48] and the unusual linear, O-bound CO_2 molecule, $[\{(^{Ad}ArO)_3tacn\}U(\eta^1\text{-}OCO)$ (Ad = adamantyl), is formed when an even larger ligand was used in the reaction with CO_2.[49]

In light of the exciting chemistry displayed by the U^{III} silylamide, we decided to explore the chemistry of some other simple U^{III} 'starting materials'. The uranium tris(aryloxides) $U(ODtbp)_3$ (ODtbp = 2,6-di-*tert*-butylphenoxide) and $[U(ODipp)_3]_2$ (ODipp =2,6,-diisopropylphenoxide) have been previously reported from the reaction of $U\{N(SiMe_3)_2\}_3$ with HODtbp and HODipp, respectively, but their small molecule reactivity remained relatively unexplored,[50,51] and only the molecular structure of the dimeric Dipp compound had been reported.[52] Herein, we show the CO coupling reaction can be generalized to tris(aryloxide) complexes, both $U(ODtbp)_3$ and the new tri-*tert*-butyl analogue $U(OTtbp)_3$ (OTtbp = 2,4,6-tri-*tert*-butylphenoxide), and that these systems exhibit other small molecule binding, namely the binding of N_2. We also report the reactivity of related alkyls and amides $U\{CH(SiMe_3)_2\}_3$ and $U\{N(SiPhMe_2)_2\}_3$ toward CO, and of $U(ODtbp)_3$, $U(OTtbp)_3$, and $U\{N(SiMe_3)_2\}_3$ toward CO_2. To yield further insight into the U−small molecule interactions, key features of the electronic and geometric structures are explored using DFT and QTAIM calculations.

RESULTS AND DISCUSSION

Dinitrogen Binding and Activation by $U(OAr)_3$ Complexes. The synthesis of $U(ODtbp)_3$ **1** has previously been described;[52] made from UN''_3 ($N'' = N(SiMe_3)_2$), and in the absence of an X-ray-determined crystal structure, was attributed a monomeric structure, in contrast to the structure of $\{U(ODipp)_3\}_2$ made by the same authors, which forms a dimer with η^6-arene coordination to U^{III}, depicted in Scheme 1.[52] In our hands, the

dx.doi.org/10.1021/ja2019492 |J. Am. Chem. Soc. 2011, 133, 9036–9051

Scheme 1. Dinitrogen Binding by $U(OAr)_3$

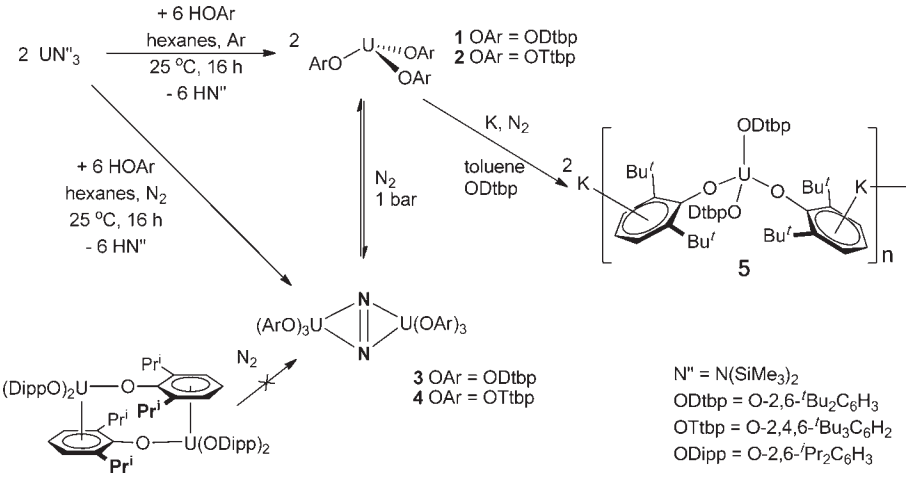

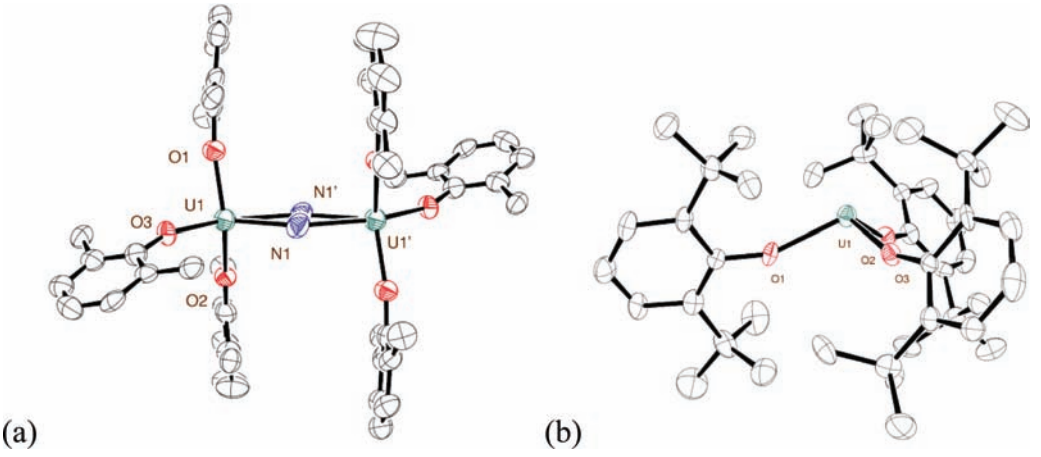

Figure 1. Thermal ellipsoid plot for (a) $[U(ODtbp)_3]_2(\mu\text{-}\eta^2\text{:}\eta^2\text{-}N_2)$ **3** crystallized from hexane; probability 50%, Me groups and lattice solvent omitted for clarity. (b) Thermal ellipsoid plot for $U(ODtbp)_3$ **1** crystallized from toluene; probability 50%. Only one independent molecule in the asymmetric unit (out of the three for **3**, and out of two for **1**) is shown. Symmetry operator used to generate symmetry generated atoms for **3**: $-x, -y+1, -z+1$.

reaction of di-*tert*-butylphenol with UN''_3 in hexane yields a dark, green-black precipitate as described in the original manuscript, and a saturated brown hexane supernatant, from which a small number of red crystals were obtained after it had been decanted into a separate vessel. An X-ray crystallographic study of these red crystals revealed the complex to be a dinitrogen-coordinated dimer $[U(ODtbp)_3]_2(\mu\text{-}\eta^2\text{:}\eta^2\text{-}N_2)$ **3**, Figure 1a, rather than the anticipated monomeric $U(ODtbp)_3$ complex **1**, in which the general structural parameters are consistent with the reduction of the side-on bound N_2 molecule to a diazenido unit by the two U^{III} cations, resulting in a nominally five-coordinate $U^{IV}(N_2)^{2-}$ dimer.

This observation caused us to study further the reaction that affords $U(ODtbp)_3$. The less soluble, dark green-black material which precipitates during the synthesis was recrystallized from either *n*-hexane or toluene solution and identified as monomeric $U(ODtbp)_3$ **1** by crystallography, Figure 1b. Investigation of the same bulk product of the reaction using powder diffraction (see Supporting Information), prior to this recrystallization confirmed that monomeric $U(ODtbp)_3$ is the major product that crystallizes from the reaction mixture, as originally suggested by Sattelberger et al. No evidence of arene-binding has been observed for **1**, but the synthesis and characterization of the solvate $(thf)U(ODtbp)_3$ were described in the original manuscript.

Complex **1** is isostructural from either solvent, containing nominally three-coordinate U^{III} (Figure 1b), but with three close U−C distances to methyl groups on the *ortho*-^{t}Bu substituents with the average U−C distance (3.272 Å) suggesting a stabilizing U−CH agostic interaction, similar to that shown by the pyramidal $U\{N(SiMe_3)_2\}_3$[53] and $U\{CH(SiMe_3)_2\}_3$ (3.05 and 3.09 Å U−C distances to agostic methyl carbon atoms, respectively).[54]

The *pseudo*-C_3 arrangement of the three aryloxides forms a shallow UO_3 pyramid in which the U^{III} center sits 0.81 Å away from the O_3 plane, an arrangement also seen in uranium tris(amides), and is explained by the polarized ion model.[53,55] The U−O bond lengths range from 2.149(4) to 2.165(3) Å (av. 2.159 Å), longer than the U−O distance in the U^{IV} complex $[U(ODtbp)_4]$ (2.135(4) Å).[51] Selected distances and angles are collected in Table 1.

Thus, although the N_2-bound product is only a minor component, this is still an unusual case of N_2 binding, particularly

dx.doi.org/10.1021/ja2019492 |*J. Am. Chem. Soc.* 2011, 133, 9036–9051

Table 1. Selected Bond Lengths (Å) for the Crystallographically Characterized Uranium Aryloxide Compounds U(ODtbp)$_3$ 1, [(DtbpO)$_3$U]$_2$(N$_2$) 3, and [(TtbpO)$_3$U]$_2$(N$_2$) 4

	U(OAr)$_3$ **1**				(μ-η^2,η^2-N$_2$) **3**, **4**				
	U(ODtbp)$_3$ from hexane **1**		U(ODtbp)$_3$ from toluene **1**		[(DtbpO)$_3$U]$_2$(N$_2$) from hexane **3**				
molecule	A	B	A	B	A	B	C	[(TtbpO)$_3$U]$_2$(N$_2$) from hexane **4**	[(TtbpO)$_3$U]$_2$(N$_2$) from toluene **4**
U−O$_{Ar}$	2.151(3)	2.161(3)	2.149(4)	2.158(5)	2.120(6)	2.123(7)	2.144(6)	2.095(6)	2.110(2)
	2.157(3)	2.165(3)	2.156(5)	2.161(5)	2.165(6)	2.156(7)	2.150(10)	2.146(6)	2.144(2)
	2.164(3)	2.165(3)	2.161(4)	2.164(4)	2.176(7)	2.166(6)	2.175(9)	2.170(6)	2.151(2)
U−O$_{Ar\ (av.)}$	2.157	2.164	2.155	2.161	2.154	2.148	2.156	2.137	2.135
U−O$_{Ar\ (av.)}$	2.159				2.152				
U−N$_1$					2.393(11)	2.389(10)	2.396(10)	2.413(9)	2.386(3)
U−N$_2$					2.393(10)	2.440(10)	2.430(10)	2.410(9)	2.423(3)
U−N$_{(av.)}$					2.393	2.415	2.413		
U−N$_{(av.)}$					2.407			2.411	2.410
N≡N					1.163(19)	1.204(17)	1.201(19)	1.190(18)	1.236(5)
N≡N$_{(av.)}$					1.189				
U···C	3.262	3.200	3.267	3.200	3.164	3.050	3.067	3.088	3.123
	3.284	3.236	3.280	3.249					
	3.400	3.245	3.394	3.255					
U···C$_{(av.)}$	3.315	3.227	3.313	3.234					
U···C$_{(av.)}$	3.272				3.093			3.088	3.123

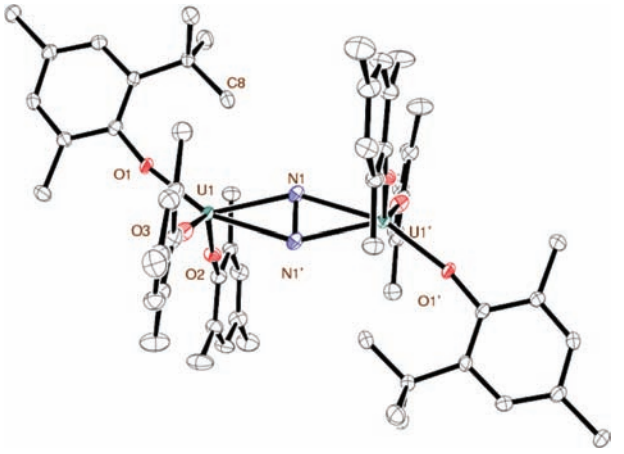

Figure 2. Thermal ellipsoid plot for [U(OTtbp)$_3$]$_2$(μ-η^2:η^2-N$_2$) **4** crystallized from toluene; probability 50%, lattice solvent and most Me groups omitted for clarity. Symmetry operator used to generate symmetry-generated atoms for **4**: $-x+1, -y+1, -z+1$.

since the reactions were carried out at ambient N$_2$ pressures, and without any particular precautions taken to retain the N$_2$. We thus investigated the scope of dinitrogen binding to uranium tris(aryloxides) by the synthesis of the new tri-*tert*-butylphenoxide analogue U(OTtbp)$_3$, which has allowed further study of dinitrogen activation.

In an analogous manner to U(ODtbp)$_3$, the reaction of UN″$_3$ with 3 equiv of HOTtbp was carried out, Scheme 1. Under argon, yellow-brown benzene solutions of U(OTtbp)$_3$ **2** are formed quantitatively overnight from UN″$_3$ and 3 equiv of HOTtbp; **2** is the same color as **1** and does not coordinate arenes. When the reaction is repeated under N$_2$ in hexane solution, dark yellow microcrystalline material is formed in high yield. Single crystals of this product, grown from either *n*-hexane or toluene, were both confirmed to be the side-on bound N$_2$ adduct [U(OTtbp)$_3$]$_2$-(μ-η^2:η^2-N$_2$) **4** by single crystal X-ray diffraction experiments, Figure 2 (with selected distances and angles in Table 1), with a molecular structure similar to that seen for **3**. The isolated yield of [U(OTtbp)$_3$]$_2$(μ-η^2:η^2-N$_2$) **4** is 80%, and N$_2$ activation appears to be quantitative according to a range of spectroscopies, even though the product is dried under dynamic vacuum.

The structures of dinitrogen-bound **3** and **4** (both solvates) are very similar, showing dinitrogen bound side-on between two uranium centers with each bound to three aryloxide ligands and with an inversion center situated between the N atoms. The N−N distances in the three independent molecules of **3** are 1.163(19), 1.204(17), and 1.201(19) Å (av. 1.189 Å), while in two molecules of **4** they are 1.190(18) Å (from *n*-hexane) and 1.236(5) Å (from toluene). The data with the smallest uncertainty in bond lengths (**4** crystallized from toluene) gave statistically significant results which are consistent with a large degree of reduction from free N$_2$ (N−N 1.0975 Å) to diazenido N$_2^{2-}$ (PhN═NPh 1.255 Å).[56] Interestingly, a close U−C contact between the uranium center and one C−H group is seen (av. 3.09 Å to C41 in **3**, 3.18 Å to C8 in **4**.toluene) which is shorter than the three contacts in U(ODtbp)$_3$.

It is instructive to compare the N−N distance in **3** and **4** to the four molecular actinide dinitrogen complexes that have been reported: the side-on bound N$_2$ in the tren complex {UN(NCH$_2$CH$_2$NSiBu^{t}Me$_2$)$_3$}$_2$(μ-η^2:η^2-N$_2$) **A** with a N−N distance 1.109(7) Å; {U(η-Cp*)(η-C$_8$H$_4${Si^{i}Pr$_3$-1,4}$_2$)}$_2$-(μ-η^2:η^2-N$_2$) **B**, N−N distance 1.232(10) Å; end-on terminal bound [{U(η-Cp*)$_3$(N$_2$)] **C**, N−N distance 1.120(14) Å; the Mo-stabilized [{C$_6$H$_3$Me$_2$-3,5}$_2$(Bu^t)N}$_3$U(μ-η^1:η^1-N$_2$)Mo-{N(Bu^t)Ph}$_3$] **D**, N−N distance 1.232(11) Å. The N═N bond length in **4** is closest to those in **B** and **D**, consistent with N$_2^{2-}$, while **A** and **C** have N−N distances indistinguishable from free N$_2$.

dx.doi.org/10.1021/ja2019492 |*J. Am. Chem. Soc.* 2011, 133, 9036–9051

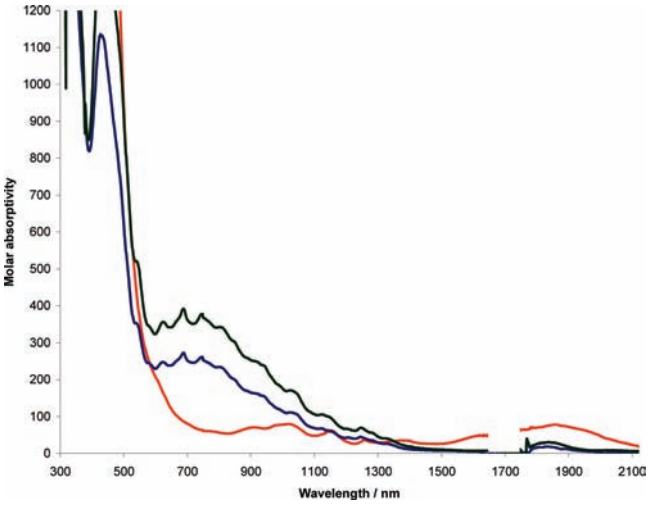

Figure 3. UV−vis−NIR spectrum $(TtbpO)_3U(N_2)U(OTtbp)_3$ **4** in toluene (red line) and of $U(OTtbp)_3$ **2** (blue line) formed from heating the solution of $(TtbpO)_3U(N_2)U(OTtbp)_3$ to 80 °C. The spectrum of $U(ODtbp)_3$ **1** (green line) is also overlaid. Lines arising from incomplete solvent subtraction around 1700 cm^{-1} have been omitted.

Comparable lanthanide-N_2 systems are $Cp^*_2Ln(N_2)LnCp^*_2$, with N−N bond lengths of 1.259(4) Å (Ln = Tm),[18] and 1.088(12) Å (Ln = Sm).[17] We return to the significance of the N−N bond length in the discussion of our calculations below.

There are notable differences in the position of the equilibrium of N_2-coordination by **3** and **4**. For the other f-element N_2 complexes described above, equilibria in solution are generally observed and these are affected by increasing the pressure of N_2. However, no loss of N_2 from **4** is observed after freeze−pump−thaw degassing a solution, and N_2 coordination is maintained under vacuum in the solid state, or when THF is added to the sample, which is most surprising. If the heterobimetallic Mo-containing complex is discounted, **4** appears to be the most robust uranium N_2 complex yet observed. The ^{1}H NMR spectrum of the N_2-bound compound contains approximately five very broad resonances between +22 and −26 ppm, which would be reasonable if there is a slow exchange between magnetically different aryl environments at ambient temperature. A low-temperature ^{1}H NMR spectrum of a toluene solution of **4** contains 13 resonances attributable to an asymmetric low temperature structure like that found in the X-ray study (see the Supporting Information for a fuller interpretation), but upon heating to 80 °C (even under an atmosphere of N_2), sharp resonances for the non-N_2 bound complex are seen as N_2 is released. The ^{1}H NMR spectrum of base-free tri-*tert*-butyl complex **2** is very similar to that for **1**, containing one sharp set of ligand resonances in the region +17 to −7 ppm. This conversion to non-N_2 bound complex was confirmed by UV−vis−NIR spectroscopy: heating a toluene solution of **4** in a gastight UV−vis cell to 80 °C under N_2 for 20 min results in a modest change in color from dark yellow to brown, but a significant change in the spectrum occurs as **4** is converted to **2** (Figure 3), a spectrum which overlays very well with that of N_2-free **1**. Storage of the sample of **2** for 1 week shows no further change in the spectrum.

Raman spectroscopy was used to determine the extent of reduction to the dinitrogen ligand in **4**. A strong band at 1451 cm^{-1} is assigned as the N_2 stretch; see Supporting Information. The $^{15}N_2$ analogue of **4** was also made, and the

Table 2. Selected Experimental (4) and Computational Data for $[U(OPh)_3]_2(\mu\text{-}\eta^2\text{:}\eta^2\text{-}N_2)$ and Free N_2 (B3LYP unless stated)[a]

r(N−N)/Å	expt	1.190, 1.236
	calcd PBE	1.303
	calcd	1.255
	calcd (free N_2)	1.104
σ(N−N)/cm^{-1}	expt	1451
	calcd PBE	1237
	calcd	1486
	calcd (free N_2)	2454
r(U−N) ave/Å	expt	2.407
	calcd	2.398
ρ (electron density)	U−N av.	0.073
	U−O av.	0.112
	N−N	0.461
	N−N (free N_2)	0.661
$\nabla^2\rho$ (electron density Laplacian)	U−N av.	0.214
	U−O av.	0.489
	N−N	−0.974
	N−N (N_2)	−2.021
H (energy density)	U−N av.	−0.010
	U−O av.	−0.003
	N−N	−0.558
	N−N (N_2)	−1.057

[a] ρ, $\nabla^2\rho$, and H data obtained at bond critical points.

Raman spectrum of ^{15}N-**4** showed a stretch at 1404 cm^{-1} very similar to the predicted stretch of 1402 cm^{-1} for a harmonic oscillator. According to the literature, no Raman active band could be identified for other side-on bound uranium N_2 complexes, but an N_2 stretch of 1425 cm^{-1} was measured for $[\{(Me_3Si)_2N\}_2(thf)Y]_2(\mu\text{-}N_2)$ in agreement with the assigned NN bond order of two.[22] We attribute the significant stability of the N_2 complex possibly to the increased electron donation from the third *tert*-butyl group of the aryloxide enhancing the reducing power of the U^{III} center, but possibly more importantly to the neatly packed structure made by **4** in solution as well as in the solid state. Solutions of **4** do not react with the other, more reactive small molecules discussed below, namely CO and CO_2, until solutions are heated above the temperature at which N_2 dissociates (80 °C in toluene). For example, single crystals of **4**·toluene were grown from a saturated toluene solution of the reaction mixture between **4** and excess CO at room temperature, attributed to incomplete reaction of the N_2 compound, and no reaction with CO_2 was observed for **4** unless the mixture was heated (see below), but **2** reacts to completion with CO within hours at room temperature (still notably faster than UN''_3 reacts with CO).

In order to probe any parallels with the LnA_3/K systems described by Evans (A = N″, OAr, Cp), that can display further N_2 reduction chemistry, $U(ODtbp)_3$ was treated with an excess of K metal in toluene under N_2 at ambient temperature with rigorous exclusion of donor solvents such as THF. A red crystalline solid formed in the resulting brown solution that could not be separated from the excess potassium and was insoluble in hydrocarbon solvents. The identity of the product was determined by X-ray crystallography to contain no coordinated N_2, but instead the U^{III} 'ate' complex $K[U(ODtbp)_4]$, which forms a polymeric chain in the solid state, in which

dx.doi.org/10.1021/ja2019492 |*J. Am. Chem. Soc.* 2011, 133, 9036–9051

Table 3. Selected Bond Lengths (Å) for the Crystallographically Characterized Uranium Aryloxide Compounds $K[U(ODtbp)_4]_n$ 5, $[(DtbpO)_3UOC]_2$ 6, $[(TtbpO)_3UOC]_2$ 7, and $(TtbpO)_4U_2(\mu\text{-}O)(\mu\text{-}O_2COTtbp)_2$ 9

	$K[U(ODtbp)_4]_n$ from toluene **5**	$[(DtbpO)_3UOC]_2$ from toluene **6**	$[(DtbpO)_3UOC]_2$ from benzene **6**	$[(TtbpO)_3UOC]_2$ from toluene **7**	$(TtbpO)_4U_2(\mu\text{-}O)(\mu\text{-}O_2COTtbp)_2$ **9**
$U-O_{Ar}$	2.244(4)	2.098(5)	2.102(3)	2.104(6)	2.132(6)
	2.251(4)	2.108(5)	2.111(3)		2.146(7)
	2.274(4)	2.112(5)	2.115(3)		
	2.321(4)				
$U-O_{Ar\ (av.)}$	2.273	2.106	2.109	2.104	2.139
U−OCC		2.120(5)	2.112(3)	2.132(9)	
C≡C		1.147(15)	1.185(9)	1.27(2)	
C−O		1.307(8)	1.298(6)	1.237(14)	
$U-\mu-O$					2.095(3)
$U-O_{carboxylate}$					2.315(7)
					2.371(7)
$UO-C_{carboxylate}$					1.258(12)
					1.253(13)
$C-OAr_{carboxylate}$					1.336(12)
$K1\cdots C_{(av.)}$	3.137				
$K1-Ar_{centroid}$	2.806				
$K2\cdots C_{(av.)}$	3.087				
$K2-Ar_{centroid}$	2.749				

$[U(ODtbp)_4]$ anions are linked through two η^6-arene interactions to a potassium cation on each side. The molecular structure is shown in the Supporting Information, with selected distances and angles collected in Table 2. The uranium center is four-coordinate with U−O bond lengths ranging from 2.244(4) to 2.321(4) Å (av. 2.273 Å) which are significantly longer than those seen in **1** (av. 2.159 Å) and in the uranium(IV) analogue $[U(ODtbp)_4]$ (2.135(4) Å).[51] The potassium−arene interaction is symmetrical with respect to the center of the arene rings (av. K−C 3.112 Å, $K-arene_{centroid}$ 2.806 and 2.749 Å), a little shorter than other K−C contacts in η^6-arene coordination previously observed (mean 3.285 Å).[57] This result is similar to the reduction of $[U\{N(SiMe_3)_2\}_3]$ with potassium in thf that generated $[K(thf)_6][U\{N(SiMe_3)_2\}_4]$.[21]

Previous DFT calculations by one of us identified $U\rightarrow N_2$ backbonding as the only covalent $U-N_2$ interaction in **A**,[58,59] and we have here performed further DFT calculations on $[U(OPh)_3]_2(\mu\text{-}\eta^2\text{:}\eta^2\text{-}N_2)$ as a model for **3** and **4**, within the constraint of C_i symmetry. Initially, three different spin states were investigated using the PBE functional; quintet, septet, and nonet, corresponding to formal uranium oxidation states of IV, III, and II, respectively. The ^5A_g state (i.e., $(U^{IV})_2(N_2^{2-})$) is clearly the ground state, 155.8 kJ mol^{-1} and 285.6 kJ mol^{-1}, respectively, more stable than the ^7A_u and ^9A_g states. The N−N distance of the PBE ^5A_g state (1.303 Å, Table 2), however, is ca. 0.1 Å longer than that observed experimentally, and the N−N stretching wavenumber (1237 cm^{-1}) smaller than that identified in the Raman spectrum of **4**, and hence the ^5A_g state was recalculated at the B3LYP level. Table 3 shows that, while the N−N stretching wavenumber and the $U-N_{ave}$ distance are now almost exactly as found experimentally, the N−N distance remains a little long. Interestingly, however, it is exactly the same as in PhN═NPh.[56]

Figure 4 shows the four highest occupied α spin MOs of the B3LYP ^5A_g state. All four clearly have significant uranium 5f content, as well as OPh ring π character. Two of the orbitals have no N_2 contribution, but the other two (HOMO-1 and HOMO-3) are π backbonding from the uranium into the N−N antibonding π_g levels. This interaction is very similar to that found previously

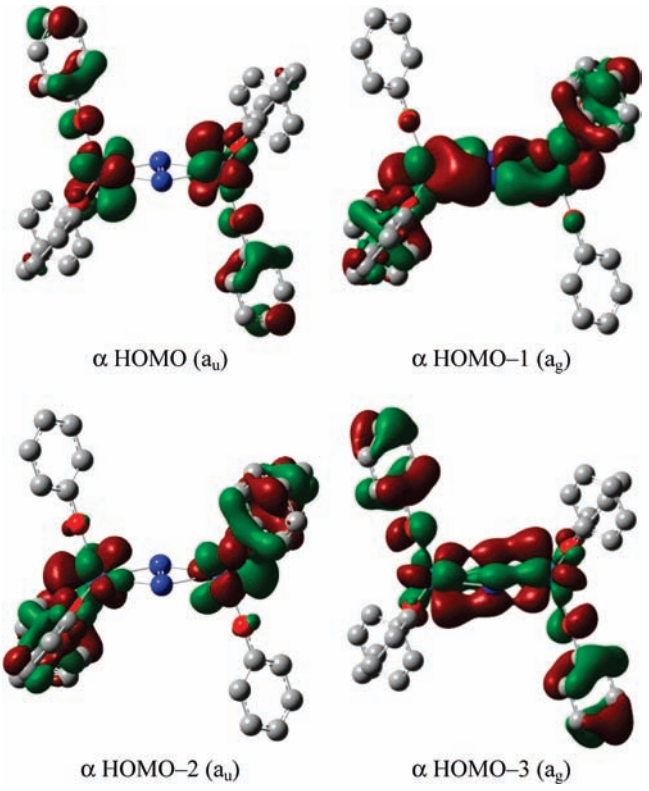

Figure 4. Representations of the four highest occupied α spin molecular orbitals in $[U(OPh)_3]_2(\mu\text{-}\eta^2\text{:}\eta^2\text{-}N_2)$ (B3LYP). H atoms omitted for clarity.

dx.doi.org/10.1021/ja2019492 |*J. Am. Chem. Soc.* 2011, 133, 9036–9051

for a model of the tren N_2 system and accounts for the lengthening of the N−N distance and reduction in vibrational wavenumber from the values for free N_2 (1.104 Å and 2454 cm^{-1}, respectively, at the present level of theory). The Hirshfeld charge of the N atoms is calculated as −0.33, in agreement with a π backbonding interaction.

Our previous calculations on the model tren−N_2 system[59,60] were performed at a time when geometry optimizations of diuranium organometallic species were not tractable. We were puzzled by the short experimental r(N−N), as the π backbonding interaction indicated by the calculations suggested strongly that the dinitrogen unit should be significantly perturbed from free N_2. We speculated that the interactions between the bulky tren ligands in the experimentally characterized compound were preventing the two ends of the molecule from moving closer together, as would be expected upon N−N lengthening and U−N shortening. Subsequent DFT study of $[U_2(\mu^2\text{-}N_2)(\eta^5\text{-}C_5H_5)_2(\eta^8\text{-}C_8H_8)_2]$,[61] in which geometry optimizations were performed, resulted in a distinct lengthening of the N−N distance from its free value, and we characterized the system as containing two U(IV) f^2 centers bridged by a N_2^{2-} ligand. This is highly reminiscent of the present calculations, and the weight of evidence now indicates that the experimental N−N distances in this type of compound are probably underestimated, to a greater or lesser extent, by the diffraction experiment, whose data are based on electron density rather than atomic position, so likely to err on the short side for a multiply bonded diatomic fragment. When comparing experiment with theory, we suggest that it is better to focus on N−N stretching wavenumber, as we have done for the first time here. As noted above, although the present B3LYP calculation of the ^5A_g ground state overestimates the experimentally determined N−N distance by ca. 0.07 Å for **3** and **4**·hexane (but slightly less for **4**·toluene), ν(N−N) matches to within 35 cm^{-1}.

We have very recently begun to apply the quantum theory of atoms-in-molecules (QTAIM)[62] to f-element organometallic complexes[63,64] and have found it to be very useful in quantifying the relative roles of ionicity and covalency. QTAIM tells us that there is one bond critical point (BCP) between each pair of atoms that are bonded to one another, and that chemical bonding interactions may be characterized and classified according to the properties of the BCPs;[65] we have focused on the electron density ρ, its Laplacian $\nabla^2\rho$, and the energy density H. Values of ρ greater than 0.2 are typical of covalent bonds, and $\nabla^2\rho$ is generally significantly less than zero for such interactions, reflecting the concentration of electron density along the bond path linking the bonded atoms. H at the BCP is negative for interactions with significant sharing of electrons, its magnitude reflecting the "covalence" of the interaction. Strongly polar bonds are characterized by low values of ρ at the BCP, together with a local charge depletion ($\nabla^2\rho > 0$).

BCP data are collected for selected bonds in ^5A_g $[U(OPh)_3]_2(\mu\text{-}\eta^2\text{:}\eta^2\text{-}N_2)$ in Table 2 (which also contains data for N_2), and the molecular graph is shown in Figure 5. This reveals BCPs between all atoms that would be expected to have a bond between them, together with ring critical points at the centers of the phenyl rings and each U−N_2 triangle. The N−N BCP data (Table 2) are typical of covalent bonds, and it is noticeable that the magnitude of ρ, $\nabla^2\rho$, and H are all less in complexed N_2 than free N_2. This is consistent with the lengthening and weakening of the N−N bond on complex formation. By contrast, the U−N and U−O BCP data indicate much less covalency, being typical of strongly polar (or indeed ionic) interactions, and very much in keeping with other U−p-block element bonds we have characterized.[63] The description of the U−N interaction as being strongly polar is consistent with population analysis of the HOMO-1 and HOMO-3, which shows that the orbitals have contributions of, respectively, 54% U f, 12% N p and 58% U f, 4% N p.

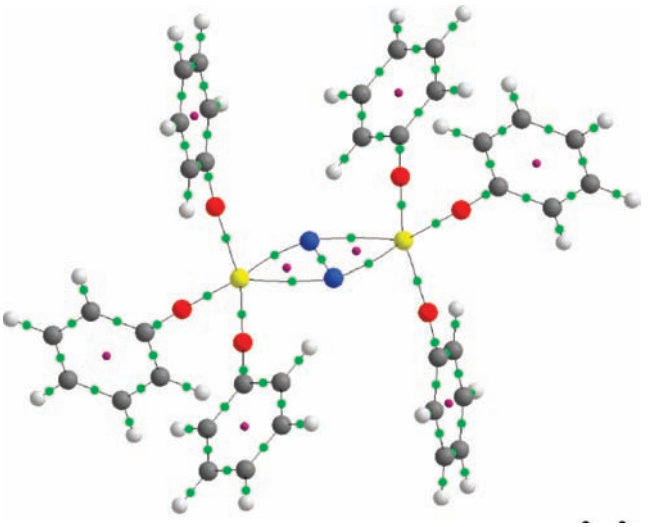

Figure 5. Molecular graph of $[U(OPh)_3]_2(\mu\text{-}\eta^2\text{:}\eta^2\text{-}N_2)$ (B3LYP). U, yellow; N, blue; O, red; C, gray; H, white; bond critical points, green; ring critical points, purple; bond paths, gray.

Discussion of N_2 Complexes. All the experimental and computational evidence collected for the N_2 complexes $[U(OAr)_3]_2(\mu\text{-}N_2)$ indicates a formal oxidation of the uranium centers to U^{IV} with concomitant reduction of the dinitrogen ligand to N_2^{2-}. The ligand exhibits a long N_2 bond length, a Raman stretch greatly reduced from free N_2, and the complexes contain weak absorptions in the UV−vis−NIR spectrum consistent with a formal U^{IV} oxidation state. The remarkable stability of **4** can then be partially attributed to these factors although the existence of **3** predominantly in its three-coordinate non N_2 bound form points to the influence of the specific aryloxide ligand as being a highly important factor. We attribute the significant stability of the N_2 complex possibly to the increased electron donation from the third *tert*-butyl group of the aryloxide enhancing the reducing power of the U^{III}, but possibly more importantly to the neatly packed structure made by **4** in solution as well as in the solid state. Solutions of **4** must be heated to eliminate N_2 forcibly before other small molecules (CO and CO_2, see below) can be activated. It is increasingly clear that experimental N−N distances in this type of compound, i.e., one containing a multiply bonded diatomic ligand, are probably underestimated by the X-ray diffraction experiment, whose data are based on electron density, giving slightly shorter N−N separations than in reality. Here, we have focused on N−N stretching wavenumber when comparing experiment with theory and propose that the N−N bond stretch should be taken as a more accurate metric for reduction than the distance. Although the present B3LYP calculation of the ^5A_g ground state here overestimates the experimentally determined N−N distance by ca. 0.07 Å, the ν(N−N) matches to within 35 cm^{-1}.

CO Binding and Coupling Using Uranium Tris(aryloxides), and Studies of CO Binding with Other Simple Homoleptic U^{III} Starting Materials. Exposure of a degassed yellow-brown toluene solution of $U(ODtbp)_3$ **1**, or the tris(tri-*tert*-butylaryloxide) analogue, $U(OTtbp)_3$ **2**, to an atmosphere of carbon monoxide

dx.doi.org/10.1021/ja2019492 |*J. Am. Chem. Soc.* 2011, 133, 9036–9051

Scheme 2. CO Binding and Coupling by $U(OAr)_3$ and $U(NR_2)_3$

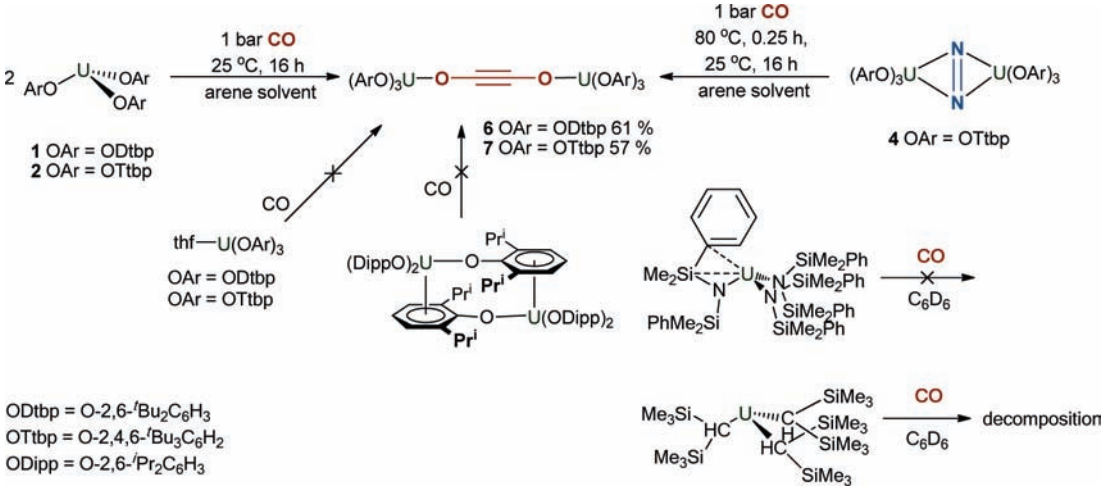

(an excess) over 16 h results in the precipitation of bright yellow microcrystals of the U^{IV} ynediolate complex, $[U(ODtbp)_3]_2(\mu\text{-}\eta^1\text{:}\eta^1\text{-}C_2O_2)$ **6**, or darker orange $[U(OTtbp)_3]_2(\mu\text{-}\eta^1\text{:}\eta^1\text{-}C_2O_2)$ **7**, Scheme 2. Both complexes have been fully characterized, and the formation is essentially quantitative. There is no indication of the formation of higher homologues of $[CO]_n^{2-}$ in the products. It is notable however that the more stable N_2 adduct **4** must be heated briefly in solution to ensure that the N_2 is fully decoordinated in order to allow the reductive CO coupling reaction to occur, because samples of **4** have been isolated from room temperature, 12 h reactions between **4** and CO in toluene. The tri-*tert*-butyl complex **7** is much less soluble than **6** in common solvents. The central alkyne carbon in **6** resonates at 0 ppm in the solution ^{13}C NMR spectrum, confirmed by comparison with that of **6a** $[U(ODtbp)_3]_2[\mu\text{-}O^{13}C^{13}CO]$ made analogously from ^{13}CO. We recently reported the synthesis of $U\{N(SiPhMe_2)_2\}_3$, an analogue of UN''_3, which has the potential to form a protective pocket from the three silyl phenyl groups around a U-coordinated small molecule;[55] the solid-state structure of the amide suggested an agostic interaction between the ipso-carbon on the SiPh group with the U. In arene solution, no reaction was observed between $U\{N(SiPhMe_2)_2\}_3$ and an excess (atmospheric pressure) of CO, even after heating to 65 °C for 24 h. We also studied the CO reactivity of the uranium tris(alkyl) complex $U\{CH(SiMe_3)_2\}_3$ which has similar agostic interactions to $U\{N(SiMe_3)_2\}_3$ between U and three silyl methyl CH groups. Upon addition of CO to a blue solution of $U\{CH(SiMe_3)_2\}_3$, the solution turned orange and ^1H NMR spectroscopy revealed the presence of $H_2C(SiMe_3)_2$ as the decomposition product.

The ynediolates **6** (two solvates) and **7** have been structurally characterized by single crystal X-ray diffraction, and the molecular structures of **6** and **7** are shown in Figure 6, with selected distances and angles collected in Table 3. First, it is clear that there is some variability in these structures with the central UOCCOU unit linear in **6**·toluene (C1A−C1−O1 angle 179.4(13)°, U1−O1−C1 angle 177.3(5)°) and **7** (C1A−C1−O1 angle 180°, U1−O1−C1 angle 180°), but slightly bent in **6**·benzene (C1A−C1−O1 angle 175.9(7)°, U1−O1−C1 angle 167.8(3)°). The C≡C bond is 1.147(15) Å in **6**·toluene and 1.185(9)° in **7**·benzene, consistent with an alkyne triple bond but it is significantly longer in **7** (1.27(2) Å), whereas the C−O bond lengths are 1.307(8) and 1.298(6) (in **6**·toluene and **6**·benzene, respectively) but shorter in **7** 1.237(14) Å although the reason for this is not readily apparent. In **6**·toluene, the U−OAr bond lengths average to 2.106 Å, in **6**·benzene they average to 2.109 Å, and in **7** they average to 2.104 Å; the U−OCC bond lengths are the same length within error for **6** (2.120(5) and 2.112(3) Å) and similar to **7** (2.132(9) Å). The U atom sits out of the O_{Ar} plane by 0.51 Å in **6**·toluene, 0.42 Å in **6**·benzene, and 0.48 Å in **7**. The parameters for **6** are very similar to those measured in $[UN''_3]_2(C_2O_2)$ ($N'' = N(SiMe_3)_2$) which has a C≡C bond length of 1.183(7) Å, an O−C bond length of 1.301(4) Å, and a U−O bond length of 2.102(2) Å.[46]

Pleasingly, both ynediolate complexes are very thermally robust. Unlike $[UN''_3]_2(C_2O_2)$, a sample of ynediolate **6** heated to 80 °C for five days neither decomposes nor reacts intramolecularly, paving the way for other intermolecular reactions of the C_2 product.

DFT calculations, without symmetry constraints, have been performed on $[U(OPh)_3CO]$ and $[U(OPh)_3CO]_2$, simplified from the experimental systems by the removal of *tert*-butyl groups. Cloke and Green suggested a mechanism in which two CO molecules bound to two uranium centers couple to form a zigzag transition state which can either react with a further molecule of CO, or rearrange to the linear ynediolate form which is no longer reactive. Likewise here, four intermediates have been located on a possible reaction pathway to form an ynediolate **IV** from a monomeric carbonyl **I**. **I** has three unpaired electrons, which mimics the first step in the experimental procedure in which neutral CO binds via C to a U^{III} f^3 center. The dinuclear molecules **II**−**IV** each have four unpaired electrons, representing electron transfer from both U centers to form U^{IV}. The geometries of the $(UCO)_n$ components of **I**−**IV** are shown in Figure 7, and their relative energies and CO vibrations are collected in Table 4. **I** has approximately C_3 symmetry while **II**−**IV** are close to C_i. The U−O−CC angle and U−O distance in **IV** (174° and 2.147 Å) are extremely close to those obtained experimentally in **6**, and the calculated C−C distance is intermediate between those found for **6** and **7**. The structures in Figure 7 are rather similar to those calculated by Cloke and Green, although the C−C distance in **II** is ca. 0.1 Å longer than for $[U(\eta\text{-COT})(\eta\text{-Cp})CO]$ while that in **III** is ca. 0.1 Å shorter. In agreement with Cloke and Green, we find that only the monomer would be

dx.doi.org/10.1021/ja2019492 |J. Am. Chem. Soc. 2011, 133, 9036–9051

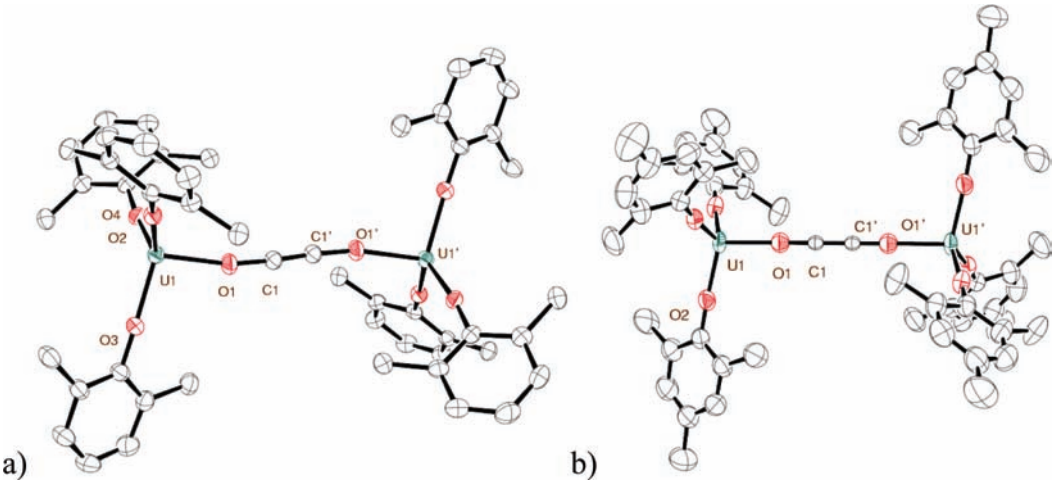

Figure 6. (a) Thermal ellipsoid plot for $[U(ODtbp)_3]_2(\mu\text{-}\eta^1\text{:}\eta^1\text{-}C_2O_2)$ **6** grown from C_6D_6. Symmetry operator used to generate symmetry generated atoms: $-x+2, -y, -z+1$. (b) Thermal ellipsoid plot for $[U(OTtbp)_3]_2(\mu\text{-}\eta^1\text{:}\eta^1\text{-}C_2O_2)$ **7**; from toluene. Symmetry operators used to generate symmetry-generated atoms: #1, $-x+y+1, -x+1, z$; #2, $-y+1, x-y, z$; #3, $-x+4/3, -y+2/3, -z-1/3$. Ellipsoid probability 50%; lattice solvent and Me groups omitted for clarity.

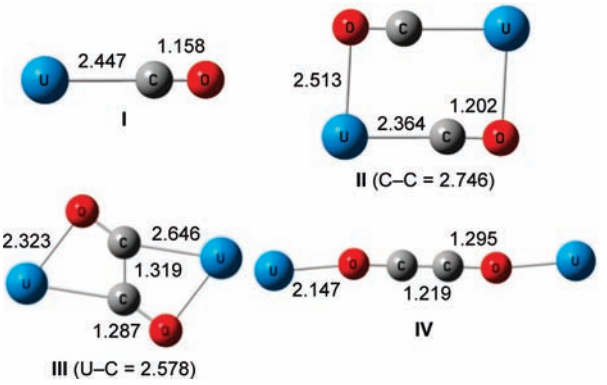

Figure 7. Calculated distances (Å) for the UCO units in **I**–**IV**.

Table 4. Relative Energies and CO Vibrations of I–IV

	I	II	III	IV
E/kJ mol^{-1}	0	−97	−149	−117
σ/cm^{-1}	1993	1721, 1665	1356	1407

expected to have an identifiable CO IR band. We also concur that the product **IV** is less stable than the intermediate **III**. Cloke and Green suggested that this may arise from neglect of the bulky substituents on the aromatic rings. Unfortunately, calculations incorporating the full aryloxide ligands are intractable.

In order to gain an estimate of which type of U–O bond in **IV** is the stronger, we have performed scans of the potential energy surfaces for lengthening one U–OAr bond and one U–OC bond from their equilibrium value, and the results are shown in Figure 8. In each case, no relaxation of the rest of the molecule was allowed, so the curves shown in Figure 8 are upper limits to the actual potential wells. Nevertheless, and although SCF convergence failures precluded extending these bonds by much more than 2 Å, it is clear that the potential well for the U–OAr interaction is much deeper, strongly suggesting that the U–OAr bond is stronger than the U–OC bond.

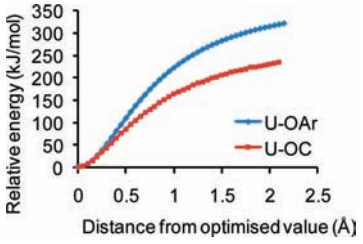

Figure 8. Relative energy of **IV** upon elongating either one U–OAr distance or one U–OC distance.

Discussion of CO Complexes. The CO coupling reaction at U^{III} that results in the formation of a $U^{IV}[(CO)_n]^{2-}U^{IV}$ fragment appears to require a fine balance between steric protection and coordinative unsaturation. Only loosely coordinated CO complexes are formed by cyclopentadienyl complexes such as $[(C_5H_5)_3U(CO)]$[39] and $[(C_5Me_5)_3U(CO)]$.[41] The presence of agostic interactions between the U^{III} center and ligand C–H bonds in $[U\{N(SiMe_3)_2\}_3]$ and $U(ODtbp)_3$ does not block the CO coordination and subsequent reductive coupling, but the η^6–arene–U interaction in $[U(ODipp)_3]_2$ and η^1–arene–U interaction in $[U\{N(SiPhMe_2)_2\}_3]$ seems sufficient to block CO binding. The aryloxides couple CO noticeably faster than UN''_3 couples CO, forming ynediolate complexes with less steric pressure, because the aryloxides can pack more effectively than silylamido ligands. The aryloxides that form $[(CO)_2]^{2-}$ complexes that are thermally stable, and not susceptible to ligand degradation, as was seen in the addition chemistry of the proximal silyl methyl group in the silylamide complexes. We cannot rule out the possibility that these latter two molecules also have lowered $U^{III/IV}$ reduction couples, but this seems unlikely to be the cause. We suggest that the ligands on the tris(alkyl) complex $U\{CH(SiMe_3)_2\}_3$ are too reactive toward CO insertion to allow a clean reductive coupling of CO in our hands; no evidence of the formation of acyl ligands from CO insertion was observed, only $CH_2(SiMe_3)_2$, the usual product of the simple thermal decomposition of $U\{CH(SiMe_3)_2\}_3$. The solvent THF blocks CO coupling for both $[U\{N(SiMe_3)_2\}_3]$ and $U(ODtbp)_3$ simply by metal coordination.

dx.doi.org/10.1021/ja2019492 |*J. Am. Chem. Soc.* 2011, 133, 9036–9051

Scheme 3. Reactions of Uranium Tris(aryloxides) with Carbon Dioxide

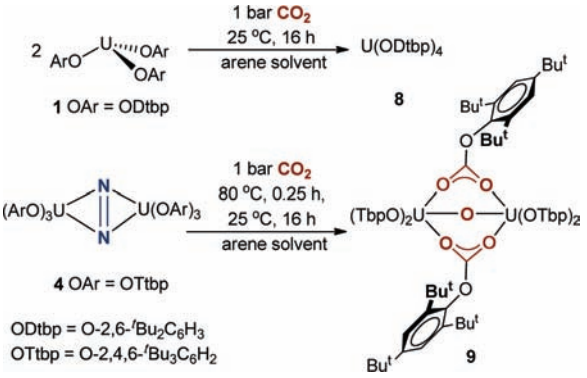

The absence of further intramolecular reaction in the $[U(OAr)_3]_2(C_2O_2)$ complexes is pleasing in that it suggests further intermolecular reactions may now be accessible for the ynediolate dianion. Particularly, as shown in Figure 8, the fact that the U−OC≡ bond is weaker than the U−OAr bond suggests a catalytic cycle could be accessible, based on the displacement of the $[OC{\equiv}CO]^{2-}$ ion and reduction of the released U^{IV} tris(aryloxide) byproduct. It has been observed that the organic diether acetylenes, ROC≡COR, are difficult to synthesize, a matter which is hampered by lower thermal stability for derivatives with smaller R groups,[66] so alternative synthetic routes would be advantageous.

Reactions of Uranium Tris(aryloxides) with Carbon Dioxide. Reactions of uranium(III) complexes with carbon dioxide have produced a number of interesting products including a terminally bound CO_2 complex[67] and two-electron reduction of CO_2 to CO,[42] as well as the formation of oxalate from two molecules of CO_2 by a Lu N_2 complex.[68] Thus, it is of interest to identify potential CO_2 chemistry with these simple tris(ligand) systems. Exposure of a benzene solution of $U(ODtbp)_3$ **1** to 1 bar of CO_2 resulted in a lightening of the color of the solution, but ^{1}H NMR spectroscopy indicated that $[U(ODtbp)_4]$ **8** was the major product arising from oxidation of the uranium center followed by ligand redistribution, Scheme 3. Again, surprisingly no reaction was observed between $[U(OTtbp)_3]_2(N_2)$ and CO_2 in benzene solutions until the temperature of the solution was elevated to allow the coordinated N_2 to be displaced. At this point, green crystalline material formed in the bottom of the flask, which proved to be very poorly soluble, similarly to the dimeric **7**. A single crystal X-ray crystallographic study revealed the identity of the complex as $(OTtbp)_2U(\mu\text{-}O)(\mu\text{-}O_2COTtbp)_2U(OTtbp)_2$ **9**, a symmetrical U^{IV} dimer resulting from U^{III} reduction of CO_2 and incorporation of the abstracted oxo atom. A further 1 equiv of CO_2 has inserted into one of the three OTtbp ligands, forming an aryl carbonate; thus, 1.5 equiv of CO_2 has been consumed per uranium. The structure is shown in Figure 9, with selected distances and angles collected in Table 3.

The U−OAr bonds are 2.132(6) and 2.146(7) Å, similar to the other distances seen. The U−μ−O distance is shorter (2.095(3) Å) and the U−O−U angle is not linear (140.4(5)°). The carbonate moiety bridges somewhat asymmetrically (U−O 2.315(7) and 2.371(7) Å) between the two U centers, and the bond lengths within the group indicate delocalization of the charge (UO−C 1.258(12) and 1.253(13) Å). The reaction between $[U(\eta\text{-}C_5Me_4H)(\eta\text{-}C_8H_4\{SiiPr_3\text{-}1,4\}_2)]$ and CO_2 was found to give a carbonate ligand which bridged between two uranium centers in a $\mu\text{-}\eta^1{:}\eta^2\text{-}CO_3$ fashion. Disorder in the carbonate unit prevents a comparison of C−O bond lengths but the η^2 U−O distances are slightly longer than those seen in **9** (2.422(10) Å).[69]

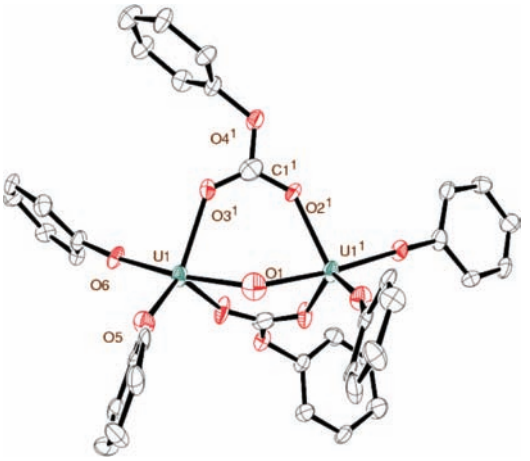

Figure 9. Thermal ellipsoid of $(OTtbp)_2U(\mu\text{-}O)(\mu\text{-}O_2COTtbp)_2U(OTtbp)_2$, **9** grown from benzene solution; probability 50%, lattice solvent and *tert*-butyl groups omitted for clarity. Symmetry operator used to generate symmetry-generated atoms: $y, x, -z$.

Finally, it is noted that the reaction of UN''_3 with CO_2 had not been discussed previously. In our hands, exposure of dark blue purple hexane solutions of UN''_3 to CO_2 (excess, atmospheric pressure) results in the formation of a pale green solution, and the precipitation of a pale green material from which toluene recrystallization affords a solid which is determined to be $U(OSiMe_3)_4$, although the ^{1}H NMR spectrum contains four magnetically inequivalent $SiMe_3$ resonances, suggesting a more complex molecular structure in solution. FTIR spectroscopic analysis of the volatiles showed a strong absorption at 2185 cm^{-1} which correlates with the formation of the isocyanate O=C=NSiMe$_3$ as an elimination product as the silylamido ligand is converted completely to a siloxide ligand, via a carbamate insertion product.

Discussion of CO_2 Complexes. The formation of a bridging oxo group has precedent in the two-electron reduction of CO_2 seen previously in uranium(III) chemistry,[47] with the assumed release of CO as a byproduct. Insertion of CO_2 into polar M−Z bonds is well-known, and hence the complex has displayed two modes of reactivity with CO_2. The lack of further CO_2 insertion into the two other U−aryloxide bonds has not been observed previously and is most likely attributable to the fact that the product crystallizes out of solution at this point. The two-electron reduction of CO_2 implies that a molecule of CO is released in the reaction. However, the flask still contains an excess of CO_2 which must react in preference to the substoichiometric CO. The conversion of silylamide to silanolate ligands via CO_2 insertion has precedent in other s- and d-block Lewis acidic metal complexes.[70]

CONCLUSIONS

U^{III} complexes which have previously been considered too sterically protected by hydrocarbyl ligand groups to coordinate further small molecules show binding and reduction of both N_2 and CO at ambient pressures, forming $[U(OAr)_3]_2(\mu\text{-}N_2)$ and $[U(OAr)_3]_2(\mu\text{-}C_2O_2)$ complexes. The kinetic inertness of the Ttbp−N_2 complex is remarkable and attributed mainly to high

dx.doi.org/10.1021/ja2019492 |J. Am. Chem. Soc. 2011, 133, 9036–9051

steric congestion; this is particularly notable in comparison to **3**, in which the bound and activated N_2 is significantly less readily captured. Metrics for di- and tri-*tert*-butylaryloxide N_2 adducts do not suggest significant differences in the reducing capability of the U^{III} centers in **1** and **2**. Uranium complexes continue to produce a range of interesting small molecule activation reactions,[32,71] particularly when the strongly reducing $U^{III/IV}$ couple is invoked.[72] Computational analysis provides strong evidence that the N_2 ligand in $[U(OAr)_3]_2(\mu\text{-}N_2)$ has indeed been reduced, and that the $(U^{IV})_2(N_2^{2-})$ formulation is appropriate. The $U-N_2$ binding is found to be strongly polar overall; the only covalent $U-N_2$ interaction is π backbonding which leads to a lengthening and weakening of the N_2 bond. We have, for the first time, been able to resolve the discrepancy between theoretical and X-ray crystallographic data for $r(N-N)$ noted in the very limited number of previous studies of uranium dinitrogen complexes, concluding that the experimental distance is an underestimation. Rather, we prefer to rely on the N−N stretching wavenumber as a better metric; the agreement between theoretical and experimental $\nu(N-N)$ is excellent and entirely in keeping with the $(U^{IV})_2(N_2^{2-})$ description.

Our experimental results show that N_2 coordination is not always easily identified and may well be prevalent in many more systems, even highly crowded f-block metal centers, than previously assumed. This would provide a pleasing explanation for the wealth of N_2-reductive functionalization shown by $[Ln\{N(SiMe_3)_2\}_3]/K$ mixtures, in which precoordination of N_2 to the Ln center could render the N_2 reducible by potassium. Despite the fact that no N_2 coordination has been observed in solution for these and related f-block complexes, the subtle differences in agostic interactions and the presence of donor solvent clearly has significant effects on the reaction outcome, as demonstrated by the difference in CO coupling reactivity by $U\{N(SiRMe_2)_2\}_3$ which is successful for R = Me but not for R = Ph. The reaction of the $U(OAr)_3$ complexes with CO_2 is more facile than that with CO and leads to a combination of CO_2 reduction and insertion at the same metal center.

We suggest that the CO coupling to form the OCCO ynediolate dianions may also be formed by many other strongly reducing f-block or early d-block complexes, opening up the coupling reaction to further chemistry of the C_2 product. Since the computational analyses of the bond strengths in the aryloxide derivatives $[U(OAr)_3]_2(\mu\text{-}C_2O_2)$ show the ynediolate fragment to be more weakly bound than the ancillary ligands, work is in progress to identify catalytic routes to functionalize and remove the OCCO fragment from the metal and close a cycle.

EXPERIMENTAL SECTION

General Details. All manipulations were carried out under a dry, oxygen-free dinitrogen, or argon where noted, atmosphere using standard Schlenk techniques or in MBraun Unilab or Vacuum Atmospheres OMNI-lab gloveboxes unless otherwise stated. THF, toluene and hexane were degassed and purified by passage through activated alumina towers prior to use. Deuterated benzene, toluene, and cyclohexane were boiled over potassium, vacuum transferred, and freeze−pump−thaw degassed three times prior to use. The compounds $U\{CH(SiMe_3)_2\}_3$,[73] $U\{N(SiMe_2Ph)_2\}_3$,[55] $U\{N(SiMe_3)_2\}_3$,[74] and $[U(ODipp)_3]_2$[52] were was made as previously described in the literature, and $U\{N(SiMe_3)_2\}_3$ was sublimed prior to use. The phenols HODtbp and HOTtbp were sublimed prior to use while all other reagents were used as purchased without further purification. ^1H and ^{13}C NMR spectra were recorded on Bruker AVA 400 or 500 MHz NMR spectrometers at 298 K. Chemical shifts are reported in parts per million and referenced to residual proton resonances calibrated against external TMS. Infrared spectra were recorded on Jasco 410 spectrophotometers. Solutions for UV−vis−NIR spectrophotometry were made in a nitrogen-filled glovebox or on a Schlenk line under argon, and spectra were recorded in a Teflon-tapped 10 mm quartz cell on a Unicam UV1 spectrophotometer. Raman spectroscopy was performed using a LabRam instrument equipped with a 50 mW He−Ne laser of wavelength 632.8 nm. Powder diffraction samples were made up in a glovebox, and the glass capillaries were flame-sealed prior to measurements being taken at room temperature on a Bruker D8 diffractometer.

Uranium(III) Aryloxides. *Slightly Improved Synthesis of U(ODtbp)$_3$* ***1*** *and Isolation of the Adduct [U(ODtbp)$_3$]$_2$(μ-η^2,η^2-N$_2$)* ***3***. *a. Under an Argon Atmosphere,* ***1***. Under an atmosphere of argon, hexane (3 cm^3, freeze−pump−thaw degassed and stored under argon) was added to a mixture of HO-2,6-$^tBu_2C_6H_3$ (161 mg, 0.78 mmol, 3.1 equiv) and $[U\{N(SiMe_3)_2\}_3]$ (181 mg, 0.25 mmol, 1 equiv) and the solution was stirred for 16 h. The suspension was allowed to settle, and a green/black precipitate was isolated from the brown supernatant by cannula filtration, washed with hexane (3 cm^3), and dried under vacuum to yield base-free $U(ODtbp)_3$ **1** (174 mg, 0.20 mmol, 80% yield). The C_6D_6 NMR solvent was freeze−pump−thaw degassed and refilled with argon before transfer onto the solid sample of **1** which was then sealed in a Youngs Teflon-valved NMR tube under argon. Characterization data agree with the literature.[52] ^1H NMR (400 MHz, 298 K, C_6D_6) δ (ppm) 16.65 (d, $^3J_{HH}$ = 7.9 Hz, 6 H, meta Ar-H), 13.75 (t, $^3J_{HH}$ = 7.2 Hz, 3 H, para Ar-H), −6.21 (s, 54 H, ^{t}Bu).

b. Under a Dinitrogen Atmosphere, ***1*** *and* ***3***. Under an atmosphere of dinitrogen, a solution of HO-2,6-$^tBu_2C_6H_3$ (1.797 g, 8.71 mmol, 3.1 equiv) in hexane (10 cm^3) was added to a solution of $[U\{N(SiMe_3)_2\}_3]$ (2.020 g, 2.81 mmol, 1 equiv) in hexane (10 cm^3) and the solution was stirred for 16 h. Stirring was then ceased, the dark black/green precipitate was allowed to settle, and the supernatant brown solution was removed by cannula filtration. The precipitate was then washed with hexane (10 cm^3) at −10 °C, and the product, base-free $U(ODtbp)_3$ **1** was dried under vacuum (2.051 g, 2.40 mmol, 85% yield). Single crystals suitable for an X-ray diffraction experiment were grown from a solution of **1** in hexanes at room temperature and also from a solution of **1** in toluene at −30 °C. Powder diffraction measurements showed that the bulk material which precipitated from hexane is pure $U(ODtbp)_3$. ^1H NMR (400 MHz, 298 K, C_6D_6) δ (ppm) 16.68 (d, $^3J_{HH}$ = 8.3 Hz, 6 H, meta Ar-H), 13.78 (t, $^3J_{HH}$ = 8.2 Hz, 3 H, para Ar-H), −6.22 (s, 54 H, ^{t}Bu). No change was observed after freeze−pump−thaw degassing of the sample. ^{13}C NMR (101 MHz, 298 K, C_6D_6) δ (ppm) 210.4 (ipso O-Ar), 182.3 (ortho Ar), 138.9 (meta Ar), 129.2 (para Ar), 8.4 (CMe_3), −60.8 (CMe_3). ^1H NMR (400 MHz, 298 K, C_6D_{12}) δ (ppm) 16.53 (d, $^3J_{HH}$ = 8.3 Hz, 6 H, meta Ar-H), 13.49 (t, $^3J_{HH}$ = 8.1 Hz, 3 H, para Ar-H), −6.61 (s, 54 H, ^{t}Bu). No change upon freeze−pump−thaw degassing. μ_{eff} (Evans NMR method) 3.3 μ_B. Mp: 195 °C.

A small number of red crystals grown from the supernatant liquors of reactions in hexanes under dinitrogen were also isolated and identified as the N_2 adduct $[U(ODtbp)_3]_2(\mu\text{-}\eta^2,\eta^2\text{-}N_2)$ **3**.

Synthesis of U(OTtbp)$_3$ ***2*** *and the Adduct [U(OTtbp)$_3$]$_2$(μ-η^2,η^2-N$_2$)* ***4***. *a. Under an Argon Atmosphere,* ***2***. Under an atmosphere of argon, C_6D_6 (0.7 cm^3, freeze−pump−thaw degassed and stored under argon) was added to HO-2,4,6-$^tBu_3C_6H_2$ (20 mg, 0.077 mmol, 3.1 equiv) and $[U\{N(SiMe_3)_2\}_3]$ (18 mg, 0.025 mmol, 1 equiv) in a Youngs Teflon-valved NMR tube and the solution was stored for 16 h, during which time dark brown/yellow $[U(OTtbp)_3]$ **2** was observed to form by ^1H NMR spectroscopy along with $HN(SiMe_3)_2$ quantitatively. ^1H NMR (400 MHz, 298 K, C_6D_6) δ (ppm) 16.82 (s, 6 H, meta Ar-H), 5.12 (s, 27 H, para ^{t}Bu), −5.87 (s, 54 H, ortho ^{t}Bu).

b. Under a Dinitrogen Atmosphere, ***4***. Under an atmosphere of dinitrogen, a solution of HO-2,4,6-$^tBu_3C_6H_2$ (1.640 g, 6.25 mmol, 3.1 equiv) in hexane (10 cm^3) was added to a solution of $[U\{N(SiMe_3)_2\}_3]$ (1.459 g, 2.03 mmol, 1 equiv) in hexane (10 cm^3) and the solution was left for 16 h. The brown supernatant solution was removed by cannula

filtration, the dark yellow crystalline solid was then washed with hexane (2 × 10 cm^3), and the product, identified as [U(OTtbp)$_3$]$_2$(μ-η^2,η^2-N$_2$) **4**, was dried under vacuum (1.682 g, 0.81 mmol, 80% yield). Single crystals suitable for an X-ray diffraction experiment were grown from a solution of **4** in either hexane or toluene at room temperature. ^{1}H NMR (400 MHz, 298 K, C$_7$D$_8$) δ (ppm) very broad signals: 21.9 (bs), −1.2 (bs), −26.9 (bs). ^{1}H NMR (400 MHz, 333 K, C$_7$D$_8$) δ (ppm) 10.7 (bs), 2.5 (bs), −7.0 (bs). Small resonances for U(OTtbp)$_3$ were also observed, and by 353 K they represent the only species in solution. IR (nujol mull) cm^{-1} (intensity): 1361 (m), 1274 (w), 1219 (s), 1190 (s), 1114 (s), 916 (w), 875 (w), 849 (m), 833 (s), 820 (m), 770 (w), 748 (m), 722 (w), 537 (m). Raman (powdered sample) cm^{-1} (intensity): 1600 (1184); 1451 (1099); 1245 (870); 1190 (794). The strong band at 1451 is assigned as the N$_2$ stretch. Mp: 165−167 °C. Anal. Calcd for C$_{108}$H$_{174}$N$_2$O$_6$U$_2$: C, 62.59; H, 8.46; N, 1.35. Found: C, 62.10; H, 8.37; N, 1.43.

Freeze−thaw degassing a toluene solution of **4** resulted in no loss of N$_2$ according to ^{1}H NMR spectroscopy, and the addition of THF to the sample also resulted in no change, i.e., no binding of THF and no displacement of N$_2$.

Synthesis of [U(OTtbp)$_3$]$_2$(μ-η^2,η^2-^{15}N$_2$) ***^{15}N-4***. HO-2,4,6-^{t}Bu$_3$C$_6$H$_2$ (354 mg, 1.35 mmol, 3.1 equiv) and [U{N(SiMe$_3$)$_2$}$_3$] (313 mg, 0.435, 1 equiv) were weighed into an ampule, and degassed hexane (10 cm^3) was condensed onto the solids at −196 °C. ^{15}N-labeled dinitrogen (98%+, in excess) was then added to the vessel, and the purple solution was allowed to warm to room temperature, changing the color to brown. This was left to stand for 16 h, and the yellow-brown crystalline material was washed with hexane (5 cm^3) and dried under vacuum to afford **^{15}N-4** (292 mg, 0.141, 65%). Raman (powder) υ (intensity) (cm^{-1}): 1404 (336).

Formation of U(OTtbp)$_3$ ***2*** *by Loss of* ***N$_2$***. For NMR spectroscopic analysis in C$_6$D$_6$, samples of **4** were heated in benzene to 80 °C in order to completely dissolve the samples, which resulted in loss of coordinated N$_2$ and formation of **2** in solution. ^{1}H NMR (400 MHz, 298 K, C$_6$D$_6$) δ (ppm) 16.84 (s, 6 H, meta Ar-H), 5.14 (s, 27 H, para ^{t}Bu), −5.90 (s, 54 H, ortho ^{t}Bu). ^{13}C NMR (101 MHz, 298 K, C$_7$D$_8$) δ (ppm) 207.6 (ipso O-Ar), 182.0 (ortho Ar), 150.1 (para Ar), 135.2 (meta Ar), 38.9 (para *C*Me$_3$), 36.8 (para C*Me$_3$*), 31.0 (ortho *C*Me$_3$), −60.4 (ortho C*Me$_3$*). μ_{eff} (Evans NMR method) 3.4 μ_B per molecule.

Synthesis of K[U(ODtbp)$_4$]$_n$ ***5***. A solution of U(ODtbp)$_3$ **1** (146 mg, 0.17 mmol) in toluene (8 cm^3) was added to a vessel sealed with a Young's tap containing a potassium mirror (in excess), and the mixture was sealed under nitrogen for 48 h. A brown solution was observed along with red crystals which adhered to the potassium mirror and were insoluble in noncoordinating solvents. The structure of the crystalline product was determined to be K[U(ODtbp)$_4$]$_n$ **5** by an X-ray crystallography study on a sample of these red crystals.

CO-Coupled Uranium(IV) Aryloxides. *Synthesis of (DtbpO)$_3$UOCCOU(ODtbp)$_3$* ***6***. A brown/yellow solution of U(ODtbp)$_3$ (1.004 g, 1.17 mmol) in toluene (25 cm^3) was degassed using the freeze−pump−thaw method and carbon monoxide (>99.9% purity, atmospheric pressure, in excess) was admitted to the vessel, and the mixture was sealed and stirred for three days. Over 16 h, a bright yellow precipitate of (DtbpO)$_3$UOCCOU(ODtbp)$_3$ **6** formed as the solution lightened to bright yellow, and the reaction was stirred for a further 56 h. The precipitate was isolated by cannula filtration, washed with hexane (10 cm^3), and dried under vacuum, yielding (DtbpO)$_3$UOCCOU(ODtbp)$_3$ **6** as a bright yellow powder (468 mg, 0.265 mmol, 45%). A further crop of product was isolated from the supernatant solution by reducing the volume to ca. 8 cm^3 under reduced vacuum and storage at −30 °C for one week (171 mg, 0.36 mmol, total yield: 61%). ^{1}H NMR (400 MHz, 298 K, C$_6$D$_6$) δ (ppm) 13.91 (d, $^3J_{HH}$ = 8.4 Hz, 12 H, meta Ar-H), 10.87 (t, $^3J_{HH}$ = 8.4 Hz, 6 H, para Ar-H), −7.35 (s, 108 H, ^{t}Bu). ^{13}C NMR (101 MHz, 298 K, C$_6$D$_6$) δ (ppm) 233.1 (ipso O-Ar), 181.0 (ortho Ar), 134.6 (para Ar), 131.1 (meta Ar), 35.0 (*C*Me$_3$), −0.37 (C≡C) −5.7 (C*Me$_3$*). μ_{eff} (Evans NMR method) 4.6 μ_B per molecule, 2.3 μ_B per U center. IR (nujol mull), cm^{-1} (intensity): 1406 (s), 1262 (w), 1210 (s), 1191 (s), 1122 (m), 1099 (w), 864 (s), 820 (m). Mp: > 250 °C. Anal. Calcd for C$_{86}$H$_{126}$O$_8$U$_2$: C, 58.56; H, 7.20; N, 0. Found: C, 57.13; H, 7.33; N, 0.20. Single crystals suitable for an X-ray diffraction experiment were grown from a solution of **5** in toluene at −30 °C.

U(ODtbp)$_3$ reacts similarly with CO/H$_2$ (1:2) to give the same product, i.e., no reaction with H$_2$ was observed at ambient pressures. There was no change upon heating a solution of (DtbpO)$_3$UOCCOU(ODtbp)$_3$ for 5 days at 80 °C in C$_6$D$_6$.

Synthesis of (DtbpO)$_3$UO^{13}C^{13}COU(ODtbp)$_3$ ***^{13}C-6***. In a Youngs Teflon-valved NMR tube, a brown/yellow solution of U(ODtbp)$_3$ (24 mg, 0.028 mmol) in C$_6$D$_6$ (0.7 cm^3) was degassed using the freeze−pump−thaw method and ^{13}C labeled carbon monoxide (95% ^{13}C, atmospheric pressure) was admitted and the NMR tube was sealed. ^{13}C NMR (101 MHz, 298 K, C$_6$D$_6$) δ (ppm) 232.6 (ipso O-Ar), 180.8 (ortho Ar), 134.5 (para Ar), 131.1 (meta Ar), 35.0 (*C*Me$_3$), −0.04 (strong, C≡C) −5.6 (C*Me$_3$*).

Synthesis of (TtbpO)$_3$UOCCOU(OTtbp)$_3$ ***7***. A brown/yellow solution of (TtbpO)$_3$U(N$_2$)U(OTtbp)$_3$ **4** (304 mg, 0.147 mmol) in toluene (20 cm^3) was degassed using the freeze−pump−thaw method, carbon monoxide (>99.9% purity, atmospheric pressure, in excess) was admitted, and the vessel was sealed and heated to 80 °C briefly, before being stirred for 4 days, to maximise precipitation of the product forming a clear yellow solution with yellow crystalline solid. The solid was isolated by filtration, washed with hexane (2 × 10 cm^3), and dried under vacuum. Yield: 174 mg, 0.083 mmol, 57%. The product is insoluble in benzene or chloroform, and only very broad ^{1}H nuclear magnetic resonances were observed in pyridine solution. Single crystals suitable for an X-ray diffraction experiment were grown from a solution of **7** in toluene cooled from 80 °C to room temperature.

The reaction proceeds only slightly if stored at room temperature for 16 h, without initial heating. Heating the solution to 50 °C for 50 min results in a significant conversion to product, but the reaction requires heating to 80 °C to achieve full conversion of all the starting material to **7** in a reasonable (sub-24 h) time period. ^{1}H NMR (400 MHz, 298 K, NC$_5$D$_5$) δ (ppm) 5.7 (very broad), −12.2 (extremely broad). (400 MHz, 298 K, C$_7$D$_8$) δ (ppm) 14.12 (s, 2 H), 3.78 (s, 9 H), −7.11 (s, 18 H). IR (nujol mull), cm^{-1} (intensity): 1423 (s), 1361 (s), 1220 (s), 1192 (s), 1115(s), 918 (w), 878 (w), 839 (s), 773 (w), 751 (m), 728 (m), 540 (m). Mp: > 250 °C.

Lack of Reaction of the Solvate (thf)U(ODtbp)$_3$ and CO. In a Youngs Teflon-valved NMR tube, to a brown/yellow solution of U(ODtbp)$_3$ (21 mg, 0.025 mmol) in C$_6$D$_6$ (0.7 cm^3) was added thf (0.1 cm^3, excess), forming (thf)U(ODtbp)$_3$. This solution was freeze−pump−thaw degassed, an atmosphere of carbon monoxide was admitted (an excess), and the tube was sealed and allowed to stand at room temperature. NMR spectroscopy revealed no reaction even after one week. ^{1}H NMR (400 MHz, 298 K, C$_6$D$_6$) δ (ppm) 16.00 (d, ^3J(H−H) = 7.9 Hz, 6 H, meta Ar-H), 13.32 (t, ^3J(H−H) = 7.2 Hz, 3 H, para Ar-H), −1.51 (s, 54 H, ^{t}Bu). Characterization data agree with the literature.[52] Coordinated thf resonances not observed due to exchange with unbound thf.

Lack of Reaction between [U(ODipp)$_3$]$_2$ and CO. A purple solution of [U(ODipp)$_3$]$_2$ (9.8 mg, 0.006 mmol) in C$_6$D$_6$ (0.7 cm^3) was degassed using the freeze−pump−thaw method, carbon monoxide (>99.9% purity, atmospheric pressure, in excess) was admitted, and the vessel was sealed. ^{1}H NMR spectroscopy revealed no change after 16 h or after heating the sample to 60 °C for 72 h. ^{1}H NMR (400 MHz, 298 K, C$_6$D$_6$) δ (ppm) 10.98 (d, $^3J_{HH}$ = 7.5 Hz, 6 H, meta Ar-H), 9.22 (t, $^3J_{HH}$ = 7.5 Hz, 3 H, para Ar-H), 2.07 (bs, CHMe$_2$), −1.83 (s, CHMe$_2$). Characterization data for **9** agree with the literature.[52]

Lack of Reaction between [U{N(SiPhMe$_2$)$_2$}$_3$] and CO. In a Youngs Teflon-valved NMR tube, a brown/yellow solution of [U{N(SiPhMe$_2$)$_2$}$_3$]

Table 5. Selected Crystallographic Details

	$U(ODtbp)_3$ **1** from hexane	$U(ODtbp)_3$ **1** from toluene	$[(DtbpO)_3U]_2(N_2)$ **3** from hexane	$[(TtbpO)_3U]_2(N_2)$ **4** from hexane	$[(TtbpO)_3U]_2(N_2)$ **4** from toluene
CCDC number	803905	803906	803909	803910	803911
chemical formula	$C_{42}H_{63}O_3U$	$C_{42}H_{63}O_3U$	$3(C_{84}H_{126}N_2O_6U_2)\cdot C_6H_{14}$	$C_{108}H_{174}N_2O_6U_2\cdot 2(C_6H_{14})$	$C_{108}H_{174}N_2O_6U_2\cdot 3(C_7H_8)$
formula mass	853.95	853.95	5293.96	2244.90	2348.95
crystal system	monoclinic	monoclinic	triclinic	triclinic	triclinic
a/Å	11.2943(2)	11.2779(7)	18.4831(2)	13.7019(4)	15.3745(6)
b/Å	31.7024(6)	31.7231(17)	19.2548(3)	15.5528(4)	15.5496(7)
c/Å	11.6570(2)	11.6467(5)	22.2299(3)	16.3640(5)	15.7297(9)
α/deg	90.00	90.00	77.9200(10)	62.492(3)	119.494(5)
β/deg	105.185(2)	105.190(5)	79.0490(10)	76.539(3)	90.110(4)
γ/deg	90.00	90.00	89.1150(10)	86.768(2)	107.466(4)
unit cell volume/Å^3	4028.11(13)	4021.3(4)	7592.87(18)	3002.72(15)	3071.1(3)
temperature/K	171(2)	171(2)	100(2)	100(2)	171(2)
space group	$P2_1$	$P2_1$	$P\bar{1}$	$P\bar{1}$	$P\bar{1}$
no. formula units/unit cell, Z	4	4	1	1	1
radiation type	Mo Kα	Mo Kα	Cu Kα	Cu Kα	Mo Kα
absorption coefficient, μ/mm^{-1}	4.063	4.070	9.245	7.896	2.684
no. of reflections measured	45752	44614	152225	57635	43366
no. of independent reflections	17542	16048	30135	11845	14066
R_{int}	0.0570	0.0663	0.0452	0.0771	0.1205
final R_1 values ($I > 2\sigma(I)$)	0.0238	0.0466	0.0866	0.0805	0.0372
final $wR(F^2)$ values ($I > 2\sigma(I)$)	0.0599	0.0576	0.2271	0.1631	0.0635
final R_1 values (all data)	0.0260	0.0698	0.1109	0.1087	0.0503
final $wR(F^2)$ values (all data)	0.0618	0.0670	0.2710	0.1852	0.0672
Flack parameter	0.462(4)	0.556(5)			
	$[KU(ODtbp)_4]_n$ **5** from toluene	$[(DtbpO)_3UOC]_2$ **6** from toluene	$[(DtbpO)_3UOC]_2$ **6** from benzene	$[(TtbpO)_3UOC]_2$ **7** from toluene	$(TbpO)_4U_2(\mu\text{-}O)(\mu\text{-}O_2COTtbp)_2$ **9**
CCDC number	814203	803907	804073	803908	814204
chemical formula	$C_{56}H_{84}KO_4U\cdot 1/2(C_7H_8)$	$C_{86}H_{126}O_8U_2\cdot 2(C_7H_8)$	$C_{86}H_{126}O_8U_2\cdot 5(C_6H_6)$	$C_{110}H_{174}O_8U_2\cdot 3(C_7H_8)$	$C_{110}H_{174}O_{11}U_2\cdot 2(C_6H_6)$
formula mass	1143.43	1948.20	2154.47	2376.95	2304.77
crystal system	triclinic	monoclinic	monoclinic	trigonal	trigonal
a/Å	11.814(2)	14.1939(6)	14.1571(4)	23.8357(12)	16.3129(4)
b/Å	12.271(3)	21.5647(9)	27.4870 (7)	23.8357(12)	16.3129(4)
c/Å	20.781(4)	18.0645(7)	14.3715 (4)	18.9486(17)	38.4536(15)
α/deg	93.065(16)	90.00	90.00	90.00	90
β/deg	99.900(16)	95.800(4)	105.898 (3)	90.00	90
γ/deg	105.924(19)	90.00	90.00	120.00	120
unit cell volume/Å^3	2837.9(10)	5501.0(4)	5378.6 (3)	9323.2(11)	8862.0(5)
temperature/K	171(2)	171(2)	171(2)	171(2)	171(2)
space group	$P\bar{1}$	$P2_1/n$	$P2_1/n$	$R\bar{3}$	$P3_221$
no. formula units/unit cell, Z	2	2	2	3	3
radiation type	Mo Kα	Mo Kα	Mo Kα	Mo Kα	Mo Kα
absorption coefficient, μ/mm^{-1}	2.975	2.985	3.06	2.654	2.792
no. of reflections measured	33520	51145	57034	79453	90056
no. of independent reflections	10713	11241	10979	4217	11216
R_{int}	0.0818	0.0254	0.041	0.0452	0.0665
final R_1 values ($I > 2\sigma(I)$)	0.0486	0.0432	0.0408	0.0764	0.0590
final $wR(F^2)$ values ($I > 2\sigma(I)$)	0.0950	0.1608	0.0895	0.1539	0.1313
Final R_1 values (all data)	0.0724	0.0710	0.0588	0.0822	0.0662
final $wR(F^2)$ values (all data)	0.1071	0.1666	0.0992	0.1572	0.1356
Flack parameter					0.095(11)

dx.doi.org/10.1021/ja2019492 |J. Am. Chem. Soc. 2011, 133, 9036–9051

(26 mg, 0.024 mmol) in C_6D_6 (0.7 cm^3) was freeze−pump−thaw degassed, an atmosphere of carbon monoxide was admitted (an excess), and the tube was sealed and allowed to stand at room temperature for 16 h. NMR spectroscopy revealed no reaction even after heating to 65 °C for 24 h.

Reaction between U{CH(SiMe$_3$)$_2$}$_3$ and CO. In a Youngs Teflon-valved NMR tube, a blue solution of U{CH(SiMe$_3$)$_2$}$_3$ (7 mg, 0.01 mmol) was degassed using the freeze−pump−thaw method, carbon monoxide was admitted (an excess), and the tube was sealed. ^{1}H NMR spectroscopy revealed disappearance of the signals due to U{CH(SiMe$_3$)$_2$}$_3$ and appearance of signals identified as $H_2C(SiMe_3)_2$ arising from decomposition. ^{1}H NMR (400 MHz, 298 K, C_6D_6) δ (ppm) 0.06 (s, 18 H, $SiMe_3$), −0.36 (s, 2 H, H_2C).

Reaction of U(ODtbp)$_3$ with CO$_2$. Synthesis of [U(ODtbp)$_4$]. A purple solution of [U(ODtbp)$_3$] **1** (12.7 mg, 0.015 mol) in C_6D_6 (0.7 cm^3) was degassed using the freeze−pump−thaw method, carbon dioxide (>99.9% purity, 1 bar pressure, in excess) was admitted, and the vessel was sealed. After 16 h, ^{1}H NMR spectroscopy revealed the formation of [U(ODtbp)$_4$] **8** as the major product. ^{1}H NMR (400 MHz, 298 K, C_6D_6) δ (ppm) 10.57 (d, $^3J_{HH}$ = 8.3 Hz, 8 H, meta Ar-H), 8.36 (t, $^3J_{HH}$ = 8.3 Hz, 4 H, para Ar-H), −0.97 (s, 72 H, CMe_3). Characterization data for [U(ODtbp)$_4$] agree with the literature.[51]

Synthesis of (TtbpO)$_2$U(μ-O)(μ-O$_2$COTtbp)$_2$U(OTtbp)$_2$ ***9***. A brown/yellow solution of [(TtbpO)$_3$U]$_2$(N_2) **4** (152 mg, 0.073 mmol) in toluene (8 cm^3) was degassed using the freeze−pump−thaw method, carbon dioxide (>99.9% purity, 1 bar pressure, in excess) was admitted, and the vessel was sealed and heated to 100 °C briefly, before being left to stand for 4 days, forming a pale brown solution with green solid. The solid was isolated by filtration, washed with hexane (2 × 10 cm^3), and dried under vacuum. Yield: 45 mg, 0.021 mmol, 29%. The product is insoluble in benzene or thf. Single crystals suitable for an X-ray diffraction experiment were grown from an analogous reaction in benzene.

Reaction of U{N(SiMe$_3$)$_2$}$_3$ with CO$_2$. Synthesis of U(OSiMe$_3$)$_4$. To a freeze-pump-thaw degassed solution of UN″$_3$ (0.30 g, 0.42 mmol) in toluene (10 mL) was added CO_2 (1 atm) to afford a clear, pale green solution. The volatiles were removed in vacuo and recrystallization from toluene at −20 °C afforded a pale green powder characterized as U($OSiMe_3$)$_4$ by empirical formula. ^{1}H NMR (C_6D_6, 500 MHz): 38.36 (9 H, s), 29.24 (3H, s), 8.67 (9 H, s), −42.86 (6 H, s), −52.02 (9 H, s) ppm. Anal. Found (calcd for $C_{12}H_{36}O_4Si_4U_1$): C, 24.18 (24.23); H, 6.03 (6.10). IR (nujol mull) cm^{-1} (intensity) 2185 (s).

Reaction of U{N(SiPhMe$_2$)$_2$}$_3$ with CO$_2$. As above, the reaction of a benzene solution of [U{N($SiPhMe_2$)$_2$}$_3$] with carbon dioxide at atmospheric pressure results in the precipitation of the uranium-containing products as a pale green solid. No further analyses were carried out.

Computational Details. Density functional theory calculations were carried out on the CO complexes using the TPSSh hybrid functional,[75] as implemented in the Gaussian 09 Rev. A.02 (G09)[76] quantum chemistry code. For the N_2 complex, both PBE[77] and B3LYP[78] functionals were employed, as discussed in the main text. A (14s 13p 10d 8f)/[10s 9p 5d 4f] segmented valence basis set with Stuttgart−Bonn variety relativistic effective core potential was used for U.[79] Dunning's cc pVDZ basis sets were employed for the non f elements. Spin-unrestricted calculations were performed on all target molecules. Wave function stability was confirmed, and spin-contamination was verified as minimal (all deviations from the ideal values of $\langle S^2 \rangle$ were less than 0.001). Energies quoted are SCF energies, including zero point energies and thermal corrections to 298 K. The ultrafine integration grid was employed, as were the default geometry and SCF convergence criteria, unless indicated otherwise in the Supporting Information. All stationary point structures had no imaginary wavenumbers, unless indicated otherwise in the Supporting Information. As the largest of these is less than 6*i* cm^{-1}, it is assumed they arise from incompleteness in the integration grid and do not represent genuine transition state structures. Atoms-in-molecules analysis was performed using the AIMALL program,[80] version 10.12.16, using a formatted G09 checkpoint file as input.

Crystallographic Details. Crystals of (DtbpO)$_3$U(N_2)U(ODtbp)$_3$·hexane, **3**·hexane, and (TtbpO)$_3$U(N_2)U(OTtbp)$_3$·hexane, **4**·hexane, suitable for X-ray diffraction analysis were grown from saturated hexane solutions which had been cannula filtered away from the precipitate produced in the reaction mixture and had been stored at room temperature for several days. These were mounted in an inert oil and then transferred to the cold gas stream of an Oxford diffraction four-circle Supernova diffractometer employing Cu Kα radiation (λ = 1.54178 Å). Crystals of U(ODtbp)$_3$ **1** were grown from either a saturated hexane solution at room temperature or a toluene solution at −30 °C. Crystals of (TtbpO)$_3$U(N_2)-U(OTtbp)$_3$·toluene, **4**·toluene, were grown from a saturated toluene solution at room temperature (surprisingly, under an atmosphere of CO). Red crystals of K[U(ODtbp)$_4$]$_n$·toluene, **5**·toluene, were grown directly from the toluene reaction mixture of U(ODtbp)$_3$ with potassium, crystals of (DtbpO)$_3$UOCCOU(ODtbp)$_3$·toluene, **6**·toluene, from a saturated toluene solution at −30 °C, crystals of (DtbpO)$_3$UOCCOU(ODtbp)$_3$·benzene, **6**·benzene, from a saturated benzene solution at 20 °C, and crystals of (TtbpO)$_3$UOCCOU(OTtbp)$_3$·toluene **7**·toluene from a saturated toluene solution cooled slowly from 80 °C to room temperature. Green crystals of (TtbpO)$_2$U(μ-O)(μ-O$_2$COTtbp)$_2$U(OTtbp)$_2$·benzene, **9**·benzene, were grown from the benzene reaction mixture of U(OTtbp)$_3$ and CO_2. Diffraction experiments on these samples were carried out on an Oxford diffraction Excalibur four-circle diffractometer employing Mo Kα radiation (λ = 0.71073 Å).[81] The structures were solved by direct or Patterson methods and refined by least-squares on weighted F^2 values for all reflections.[82] All hydrogen atoms were constrained to ideal geometries and refined with fixed isotropic displacement parameters. Refinement proceeded to give the residuals shown in Table 5. Complex neutral-atom scattering factors were used.[83] Crystal structure data are available in cif format from www.ccdc.ac.uk, codes 803905−803911, 804073, 814203, and 814204.

The molecular structure of U(ODtbp)$_3$ **1** determined from crystals grown from both hexane and toluene solutions showed the uranium atoms to be disordered above and below the plane formed by the oxygen atoms. There were no systematic absences for a *c*-glide, and examination of the structure revealed that $P2_1$ is the correct space group, as the space group $P2_1/c$ would map the higher occupancy U position onto the low occupancy U position of the other molecule in the asymmetric unit. The structure of (DtbpO)$_3$U(N_2)U(ODtbp)$_3$·hexane **3**·hexane revealed three molecules in the asymmetric unit. One molecule of hexane solvent was modeled successfully, but the SQUEEZE routine in the PLATON suite of software identified a number more in a solvent-accessible void and was dealt with accordingly. The structure of (TtbpO)$_3$U(N_2)U(OTtbp)$_3$·hexane, **4**·hexane, has a disordered molecule of hexane which was successfully modeled. The structures of (TtbpO)$_3$U(N_2)U(OTtbp)$_3$·toluene, **4**·toluene, and (TtbpO)$_3$UOCCOU(OTtbp)$_3$·toluene, **7**·toluene, both had molecules of toluene disordered over inversion centers. The structure of K[U(ODtbp)$_4$]$_n$·toluene, **5**·toluene, has a disordered molecule of toluene and disorder of two *tert*-butyl groups which were successfully modeled. The structure of (DtbpO)$_3$UOCCOU(ODtbp)$_3$·toluene, **6**·toluene, has a disordered molecule of toluene, successfully modeled, and SQUEEZE revealed no further disordered solvate molecules even though solvent-accessible voids were identified. The structure of (TtbpO)$_2$U(μ-O)-(μ-O$_2$COTtbp)$_2$U(OTtbp)$_2$·benzene, **9**·benzene, had a disordered benzene solvate molecule in the asymmetric unit.

■ ASSOCIATED CONTENT

Supporting Information. Full crystal structure and space-filling drawings, further details for the complexes described, additional spectra and characterization data, additional computational

details and atomic coordinates, and complete ref 76. This material is available free of charge via the Internet at http://pubs.acs.org.

AUTHOR INFORMATION

Corresponding Author
polly.arnold@ed.ac.uk; n.kaltsoyannis@ucl.ac.uk

ACKNOWLEDGMENT

We thank Mr. S. Hunter and Prof. C. R. Pulham for the collection of Raman data, Drs. Ian J. Casely and Zoe R. Turner for the data for $U(OSiMe_3)_4$, the UK EPSRC (fellowship for P.L.A., funding for S.M.M.), and the University of Edinburgh for funding. We are also grateful for computing resources via the UCL Research Computing "Legion" cluster and "Unity" facility, and the UK National Service for Computational Chemistry Software (http://www.nsccs.ac.uk).

REFERENCES

(1) *Activation of Small Molecules*, 1st ed.; Tolman, W. B., Ed.; Wiley: Weinheim, 2006.
(2) Burgess, B. K.; Lowe, D. J. *Chem. Rev.* **1996**, *96*, 2983–3011.
(3) Howard, J. B.; Rees, D. C. *Proc. Natl. Acad. Sci. U.S.A.* **2006**, *103*, 17088–17093.
(4) Erisman, J. W.; Sutton, M. A.; Galloway, J.; Klimont, Z.; Winiwarter, W. *Nat. Geosci.* **2008**, *1*, 636–639.
(5) Zheng, C.; Apeloig, Y.; Hoffmann, R. *J. Am. Chem. Soc.* **1988**, *110*, 749–774.
(6) Hoffman, B. M.; Dean, D. R.; Seefeldt, L. C. *Acc. Chem. Res.* **2009**, *42*, 609–619.
(7) (a) Howard, J. B.; Rees, D. C. *Chem. Rev.* **1996**, *96*, 2965–2982. (b) Schrock, R. R. *Proc. Natl. Acad. Sci. U.S.A.* **2006**, *103*, 17087–17087.
(8) Schrock, R. R. *Nat. Chem.* **2011**, *3*, 95.
(9) Khodakov, A. Y.; Chu, W.; Fongarland, P. *Chem. Rev.* **2007**, *107*, 1692–1744.
(10) Herrmann, W. A. *Angew. Chem., Int. Ed. Engl.* **1982**, *21*, 117–130.
(11) Miller, A. J. M.; Labinger, J. A.; Bercaw, J. E. *J. Am. Chem. Soc.* **2008**, *130*, 11874–11875.
(12) (a) Ballmann, J.; Munhá, R. F.; Fryzuk, M. D. *Chem. Commun.* **2010**, *46*, 1013–1025. (b) Werkema, E. L.; Maron, L.; Eisenstein, O.; Andersen, R. A. *J. Am. Chem. Soc.* **2007**, *129*, 2529–2541.
(13) Fryzuk, M. D.; Love, J. B.; Rettig, S. J.; Young, V. G. *Science* **1997**, *275*, 1445–1447.
(14) Pool, J. A.; Lobkovsky, E.; Chirik, P. J. *Nature* **2004**, *427*, 527–530.
(15) (a) Knobloch, D. J.; Lobkovsky, E.; Chirik, P. J. *Nat. Chem.* **2010**, *2*, 30–35. (b) Knobloch, D. J.; Lobkovsky, E.; Chirik, P. J. *J. Am. Chem. Soc.* **2010**, *132*, 10553–10564.
(16) (a) Yandulov, D. V.; Schrock, R. R. *Science* **2003**, *301*, 76–78. (b) Arashiba, K.; Miyake, Y.; Nishibayashi, Y. *Nat. Chem.* **2011**, *3*, 120.
(17) Evans, W. J.; Ulibarri, T. A.; Ziller, J. W. *J. Am. Chem. Soc.* **1988**, *110*, 6877–6879.
(18) Evans, W. J.; Allen, N. T.; Ziller, J. W. *J. Am. Chem. Soc.* **2001**, *123*, 7927–7928.
(19) (a) Evans, W. J.; Allen, N. T.; Ziller, J. W. *Angew. Chem., Int. Ed.* **2002**, *41*, 359. (b) Evans, W. J.; Zucchi, G.; Ziller, J. W. *J. Am. Chem. Soc.* **2003**, *125*, 10–11.
(20) (a) Evans, W. J.; Lee, D. S.; Johnston, M. A.; Ziller, J. W. *Organometallics* **2005**, *24*, 6393–6397. (b) Evans, W. J.; Lee, D. S.; Lie, C.; Ziller, J. W. *Angew. Chem., Int. Ed.* **2004**, *43*, 5517–5519. (c) Evans, W. J.; Lee, D. S.; Ziller, J. W. *J. Am. Chem. Soc.* **2004**, *126*, 454–455. (d) Evans, W. J.; Rego, D. B.; Ziller, J. W. *Inorg. Chem.* **2006**, *45*, 10790–10798. (e) Schmiege, B. M.; Ziller, J. W.; Evans, W. J. *Inorg. Chem.* **2010**, *49*, 10506–10511.
(21) Evans, W. J.; Lee, D. S.; Rego, D. B.; Perotti, J. M.; Kozimor, S. A.; Moore, E. K.; Ziller, J. W. *J. Am. Chem. Soc.* **2004**, *126*, 14574–14582.
(22) Evans, W. J.; Fang, M.; Zucchi, G.; Furche, F.; Ziller, J. W.; Hoekstra, R. M.; Zink, J. I. *J. Am. Chem. Soc.* **2009**, *131*, 11195–11202.
(23) Fang, M.; Bates, J. E.; Lorenz, S. E.; Lee, D. S.; Rego, D. B.; Ziller, J. W.; Furche, F.; Evans, W. J. *Inorg. Chem.* **2011**, *50*, 1459.
(24) Demir, S.; Lorenz, S. E.; Fang, M.; Furche, F.; Meyer, G.; Ziller, J. W.; Evans, W. J. *J. Am. Chem. Soc.* **2010**, *132*, 11151–11158.
(25) (a) Spencer, L. P.; MacKay, B. A.; Patrick, B. O.; Fryzuk, M. D. *Proc. Natl. Acad. Sci. U. S. A.* **2006**, *103*, 17094–17098. (b) Gardiner, M. G. *Materials* **2010**, *3*, 841.
(26) Roussel, P.; Scott, P. *J. Am. Chem. Soc.* **1998**, *120*, 1070–1071.
(27) Cloke, F. G. N.; Hitchcock, P. B. *J. Am. Chem. Soc.* **2002**, *124*, 9352–9353.
(28) Evans, W. J.; Kozimor, S. A.; Ziller, J. W. *J. Am. Chem. Soc.* **2003**, *125*, 14264–14265.
(29) Odom, A. L.; Arnold, P. L.; Cummins, C. C. *J. Am. Chem. Soc.* **1998**, *120*, 5836–5837.
(30) Korobkov, I.; Gambarotta, S.; Yap, G. P. A. *Angew. Chem., Int. Ed.* **2002**, *41*, 3433–3436.
(31) Monreal, M. J.; Diaconescu, P. L. *Nat. Chem.* **2010**, *2*, 423–423.
(32) Fox, A. R.; Bart, S. C.; Meyer, K.; Cummins, C. C. *Nature* **2008**, *455*, 341–349.
(33) (a) Bianconi, P. A.; Vrtis, R. N.; Rao, C. P.; Williams, I. D.; Engeler, M. P.; Lippard, S. J. *Organometallics* **1987**, *6*, 1968–1977. (b) Bianconi, P. A.; Williams, I. D.; Engeler, M. P.; Lippard, S. J. *J. Am. Chem. Soc.* **1986**, *108*, 311–313.
(34) Vrtis, R. N.; Rao, C. P.; Bott, S. G.; Lippard, S. J. *J. Am. Chem. Soc.* **1988**, *110*, 7564–7566.
(35) Coffin, V. L.; Brennen, W.; Wayland, B. B. *J. Am. Chem. Soc.* **1988**, *110*, 6063–6069.
(36) Watanabe, T.; Ishida, Y.; Matsuo, T.; Kawaguchi, H. *J. Am. Chem. Soc.* **2009**, *131*, 3474.
(37) (a) Ellis, J. E.; Fjare, K. L.; Hayes, T. G. *J. Am. Chem. Soc.* **1981**, *103*, 6100–6106. (b) Weiss, E.; Buchner, W. *Helv. Chim. Acta* **1963**, *46*, 1121. (c) Weiss, E.; Buchner, W. *Z. Anorg. Allg. Chem.* **1964**, *330*, 251–258. (d) Buchner, W.; Weiss, E. *Helv. Chim. Acta* **1964**, *47*, 1415.
(38) Evans, W. J.; Lee, D. S.; Ziller, J. W.; Kaltsoyannis, N. *J. Am. Chem. Soc.* **2006**, *128*, 14176–14184.
(39) Brennan, J. G.; Andersen, R. A.; Robbins, J. L. *J. Am. Chem. Soc.* **1986**, *108*, 335–336.
(40) (a) Conejo, M. D.; Parry, J. S.; Carmona, E.; Schultz, M.; Brennan, J. G.; Beshouri, S. M.; Andersen, R. A.; Rogers, R. D.; Coles, S.; Hursthouse, M. *Chem.—Eur. J.* **1999**, *5*, 3000–3009. (b) Parry, J.; Carmona, E.; Coles, S.; Hursthouse, M. *J. Am. Chem. Soc.* **1995**, *117*, 2649–2650. (c) Maron, L.; Eisenstein, O.; Andersen, R. A. *Organometallics* **2009**, *28*, 3629–3635.
(41) Evans, W. J.; Kozimor, S. A.; Nyce, G. W.; Ziller, J. W. *J. Am. Chem. Soc.* **2003**, *125*, 13831–13835.
(42) Castro-Rodriguez, I.; Meyer, K. *J. Am. Chem. Soc.* **2005**, *127*, 11242–11243.
(43) Summerscales, O. T.; Cloke, F. G. N.; Hitchcock, P. B.; Green, J. C.; Hazari, N. *Science* **2006**, *311*, 829–831.
(44) Summerscales, O. T.; Cloke, F. G. N.; Hitchcock, P. B.; Green, J. C.; Hazari, N. *J. Am. Chem. Soc.* **2006**, *128*, 9602–9603.
(45) Frey, A. S.; Cloke, F. G. N.; Hitchcock, P. B.; Day, I. J.; Green, J. C.; Aitken, G. *J. Am. Chem. Soc.* **2008**, *130*, 13816–13817.
(46) Arnold, P. L.; Turner, Z. R.; Bellabarba, R. M.; Tooze, R. P. *Chem. Sci.* **2011**, *2*, 77–79.
(47) Berthet, J. C.; Lemarechal, J. F.; Nierlich, M.; Lance, M.; Vigner, J.; Ephritikhine, M. *J. Organomet. Chem.* **1991**, *408*, 335–341.
(48) Castro-Rodriguez, I.; Meyer, K. *Chem. Commun.* **2006**, 1353–1368.
(49) Castro-Rodriguez, I.; Nakai, H.; Zakharov, L. N.; Rheingold, A. L.; Meyer, K. *Science* **2004**, *305*, 1757–1759.
(50) (a) Van der Sluys, W. G.; Sattelberger, A. P. *Chem. Rev.* **1990**, *90*, 1027–1040. (b) Van der Sluys, W. G.; Sattelberger, A. P. *Inorg. Chem.* **1989**, *28*, 2496–2498.

(51) Berg, J. M.; Clark, D. L.; Huffman, J. C.; Morris, D. E.; Sattelberger, A. P.; Streib, W. E.; Vandersluys, W. G.; Watkin, J. G. *J. Am. Chem. Soc.* **1992**, *114*, 10811–10821.
(52) Van der Sluys, W. G.; Burns, C. J.; Huffman, J. C.; Sattelberger, A. P. *J. Am. Chem. Soc.* **1988**, *110*, 5924–5925.
(53) Stewart, J. L.; Andersen, R. A. *Polyhedron* **1998**, *17*, 953–958.
(54) Van der Sluys, W. G.; Burns, C. J.; Sattelberger, A. P. *Organometallics* **1989**, *8*, 855–857.
(55) Mansell, S. M.; Perandones, B. F.; Arnold, P. L. *J. Organomet. Chem.* **2010**, *695*, 2814–2821.
(56) Fryzuk, M. D.; Johnson, S. A. *Coord. Chem. Rev.* **2000**, *200*, 379–409.
(57) Search of the CSD Version 5.31, update 1.
(58) Kaltsoyannis, N.; Scott, P. *Chem. Commun.* **1998**, 1665–1666.
(59) Roussel, P.; Errington, W.; Kaltsoyannis, N.; Scott, P. *J. Organomet. Chem.* **2001**, *635*, 69–74.
(60) Kaltsoyannis, N.; Scott, P. *Chem. Commun.* **1998**, 1665.
(61) Cloke, F. G. N.; Green, J. C.; Kaltsoyannis, N. *Organometallics* **2004**, *23*, 832–835.
(62) Bader, F. *Atoms in Molecules: A Quantum Theory*; OUP: Oxford, 1990.
(63) (a) Tassell, M. J.; Kaltsoyannis, N. *Dalton Trans.* **2010**, *39*, 6719–6725. (b) Arnold, P. L.; Turner, Z. R.; Kaltsoyannis, N.; Pelekanaki, P.; Bellabarba, R. M.; Tooze, R. B. *Chem.—Eur. J.* **2010**, *16*, 9623–9629. (c) Kirker, I.; Kaltsoyannis, N. *Dalton Trans.* **2011**, *40*, 124.
(64) Saleh, L.; Birjkumar, K.; Protchenko, A.; Schwartz, A.; Aldridge, S.; Jones, C.; Kaltsoyannis, N.; Mountford, P. *J. Am. Chem. Soc.* **2011**, *133* (11), 3836–3839 .
(65) Matta, C. F.; Boyd, R. J. In *The quantum theory of atoms in molecules*; Matta, C. F., Boyd, R. J., Eds.; Wiley-VCH: Weinheim, 2007, pp 1−34.
(66) (a) Gleiter, R.; Werz, D. B.; Rominger, F.; Zhutov, E.; Zefirov, N. S.; Proskurnina, M. V. *Eur. J. Org. Chem.* **2007**, 5834–5839. (b) Gleiter, R.; Werz, D. B. *Chem. Rev.* **2010**, *110*, 4447–4488.
(67) Castro-Rodriguez, I.; Nakai, H.; Zakharov, L. N.; Rheingold, A. L.; Meyer, K. *Science* **2004**, *305*, 1757–1759.
(68) Evans, W. J.; Lorenz, S. E.; Ziller, J. W. *Inorg. Chem.* **2009**, *48*, 2001–2009.
(69) Summerscales, O. T.; Frey, A. S. P.; Cloke, F. G. N.; Hitchcock, P. B. *Chem. Commun.* **2009**, 198.
(70) Phull, H.; Alberti, D.; Korobkov, I.; Gambarotta, S.; Budzelaar, P. H. M. *Angew. Chem., Int. Ed.* **2006**, *45*, 5331–5334.
(71) (a) Monreal, M. J.; Diaconescu, P. L. *Organometallics* **2008**, *27*, 1702–1706. (b) Ephritikhine, M. *Dalton Trans.* **2006**, 2501–2516. (c) Lam, O. P.; Anthon, C.; Meyer, K. *Dalton Trans.* **2009**, 9677–9691.
(72) Evans, W. J.; Kozimor, S. A. *Coord. Chem. Rev.* **2006**, *250*, 911–935.
(73) Van der Sluys, W. G.; Burns, C. J.; Sattelberger, A. P. *Organometallics* **1989**, *8*, 855–857.
(74) Clark, D. L.; Sattelberger, A. P.; Andersen, R. A. *Inorg. Synth.* **1997**, *31*, 307.
(75) Tao, J. M.; Perdew, J. P.; Staroverov, V. N.; Scuseria, G. E. *Phys. Rev. Lett.* **2003**, *91*, 14.
(76) Frisch, M. J.; *Gaussian 09*, Revision A.2; Gaussian, Inc.: Wallingford, CT, 2009.
(77) Perdew, J. P.; Burke, K.; Ernzerhof, M. *Phys. Rev. Lett.* **1996**, *77*, 3865.
(78) Becke, A. *Phys. Rev. A* **1988**, *38*, 3098.
(79) Cao, X. Y.; Dolg, M. *J. Mol. Struct. (THEOCHEM)* **2004**, *673*, 203.
(80) Keith, T. 2011, AIMALL version 10.12.16, http://aim.tkgristmill.com/.
(81) Agilent Oxford Diffraction Ltd., Yarnton, England, 2009.
(82) Sheldrick, G. M. *Acta Crystallogr., Sect. A: Found. Crystallogr.* **2008**, *64*, 112–122.
(83) *International Tables for Crystallography*; Kluwer: Dordrecht, 1992; Vol. C.